Papahu taitapu, gen. et sp. nov., an early Miocene stem odontocete (Cetacea) from New Zealand

Aguirre-Fernández, Gabriel ; Fordyce, R Ewan

Abstract: The early Miocene is one of the least understood intervals in cetacean evolution. A new early Miocene dolphin described here, Papahu taitapu, gen. et sp. nov. (family incertae sedis, Cetacea, Odontoceti), is from the Kaipuke Formation (21.7–18.7 Ma) of North West Nelson, New Zealand. The holotype of Papahu taitapu includes a skull with an open mesorostral canal, a broad-based rostrum (broken anteriorly), two pairs of premaxillary foramina, a slight bilateral asymmetry at the antorbital notches, a slight intertemporal constriction exposing the temporal fossa and the lateral wall of the braincase in dorsal view, and single-rooted (and probably homodont) teeth. The periotic has an inflated, spherical pars cochlearis and an anterior process with the anterointernal sulcus and a recurved lateral sulcus well developed. The skull size indicates a body length of about 2 m. Papahu taitapu plots cladistically in a cluster of archaic dolphins variously referred to as Platanistoidea or as stem Odontoceti. It matches no family described so far, but cladistic relationships for comparable odontocetes are not yet resolved enough to justify family placement.

DOI: https://doi.org/10.1080/02724634.2013.799069

Journal of Vertebrate Paleontology

ISSN: 0272-4634 (Print) 1937-2809 (Online) Journal homepage: http://www.tandfonline.com/loi/ujvp20

Papahu taitapu, gen. et sp. nov., an early Miocene stem odontocete (Cetacea) from New Zealand

Gabriel Aguirre-Fernández & R. Ewan Fordyce

To cite this article: Gabriel Aguirre-Fernández & R. Ewan Fordyce (2014) Papahu taitapu, gen. et sp. nov., an early Miocene stem odontocete (Cetacea) from New Zealand, Journal of Vertebrate Paleontology, 34:1, 195-210, DOI: 10.1080/02724634.2013.799069

To link to this article: http://dx.doi.org/10.1080/02724634.2013.799069

Journal of Vertebrate Paleontology 34(1):195–210, January 2014

ARTICLE

PAPAHU TAITAPU, GEN. ET SP. NOV., AN EARLY MIOCENE STEM ODONTOCETE (CETACEA) FROM NEW ZEALAND

GABRIEL AGUIRRE-FERNÁNDEZ* and R. EWAN FORDYCE
Department of Geology, University of Otago, P.O. Box 56, Dunedin 9054, New Zealand, gabriel.aguirre@otago.ac.nz

ABSTRACT—The early Miocene is one of the least understood intervals in cetacean evolution. A new early Miocene dolphin described here, *Papahu taitapu*, gen. et sp. nov. (family incertae sedis, Cetacea, Odontoceti), is from the Kaipuke Formation (21.7–18.7 Ma) of North West Nelson, New Zealand. The holotype of *Papahu taitapu* includes a skull with an open mesorostral canal, a broad-based rostrum (broken anteriorly), two pairs of premaxillary foramina, a slight bilateral asymmetry at the antorbital notches, a slight intertemporal constriction exposing the temporal fossa and the lateral wall of the braincase in dorsal view, and single-rooted (and probably homodont) teeth. The periotic has an inflated, spherical pars cochlearis and an anterior process with the anterointernal sulcus and a recurved lateral sulcus well developed. The skull size indicates a body length of about 2 m. *Papahu taitapu* plots cladistically in a cluster of archaic dolphins variously referred to as Platanistoidea or as stem Odontoceti. It matches no family described so far, but cladistic relationships for comparable odontocetes are not yet resolved enough to justify family placement.

SUPPLEMENTAL DATA—Supplemental materials are available for this article for free at www.tandfonline.com/UJVP

INTRODUCTION

The reported record of early Miocene Odontoceti (Cetacea) implies a high taxonomic diversity, consistent with the idea that odontocetes started to radiate during the Oligocene and peaked in diversity in the middle to late Miocene (Uhen and Pyenson, 2007; Marx and Uhen, 2010). Opinions vary on the number and content of families of early Miocene odontocetes, but recent authors have listed up to 10 families, and/or additional stem clusters, attributed to four superfamilies: (1) Platanistoidea (sensu Muizon, 1987, variously including Dalpiazinidae, Squalodelphinidae, Squalodontidae, Prosqualodontidae, and Allodelphinidae); (2) Eurhinodelphinoidea (sensu Muizon, 1991, with Eoplatanistidae and Eurhinodelphinidae); (3) Physeteroidea (sensu Lambert, 2008, variously including Kogiidae and Physeteridae); and (4) Delphinoidea (sensu Muizon, 1988a, with Kentriodontidae). This seemingly high early Miocene family-level diversity is somewhat illusory: the families are represented by few genera and species, with some species known from a single fossil. Further, use of the early Miocene as a single time 'bin' masks both the general global rarity of Cetacea of Aquitanian age (23.03–20.43 Ma), and problems of dating. Of the two most widely cited early Miocene assemblages, the Patagonian fauna from Argentina is Burdigalian (Cione et al., 2011). The Belluno fauna (Libano Sandstone, Italy) has not been directly dated by pelagic microfossils, but was considered by Bianucci and Landini (2002:22), who noted that it "may be upper Aquitanian or/and lower Burdigalian in age ... we consider it probable that the cetacean fauna, given its archaism, can be entirely included within the Aquitanian." To consider phylogenetic placement for the families above, the relationships of Delphinoidea are relatively uncontentious, but Physeteroidea and Platanistoidea have more complex phylogenetic and taxonomic histories (Lambert, 2005; Lee et al., 2012). Geisler and Sanders (2003; see also Geisler et al., 2011, 2012) used a large data set of morphological characters and provided an alternative hypothesis to the widely accepted concept of Platanistoidea proposed by Muizon (1987), but relationships remain uncertain (Uhen et al., 2008; Murakami et al., 2012). The enigmatic Eurhinodelphinoidea has been tentatively placed as a sister clade to Delphinida (Muizon, 1991) and Ziphiidae (Lambert, 2005), but its affinities are poorly understood (Fordyce and Muizon, 2001).

Problems of systematics summarized above can be resolved only by documenting new material. This article describes a new genus and species of odontocete from the Kaipuke Formation (Otaian local stage, middle Aquitanian to middle Burdigalian, early Miocene) of New Zealand. The material includes a reasonably complete skull (lacking the anterior part of the rostrum), a periotic, a mandible, and some postcranial material.

The article includes a cladistic analysis based on the morphological partition of a published combined matrix (Geisler et al., 2012) to reveal the relationships of the Kaipuke Formation specimen among the Odontoceti.

METHODOLOGY

Preparation, Anatomical Description, and Illustration

The fossil was prepared mechanically (with pneumatic scribes, and some air-abrasive etching) and chemically (with acetic acid, 5%). Fine preparation of sutures was performed under a Zeiss binocular microscope with 8–20× magnification.

Anatomical terminology generally follows Mead and Fordyce (2009). Most specimens were coated with sublimed ammonium chloride for photography. All photographs were taken using a Nikon D700 camera body and a Nikon 105 mm f/2.8 micro lens. Specimens were lighted from the upper left. Sketch in Figure 6B was drawn using a camera lucida attached to a binocular microscope.

For skull orientations in images, we used the condylobasal axis (tip of rostrum to posterior border of condyles) as the

*Corresponding author.

horizontal axis and a line perpendicular to the condylobasal axis as the vertical axis.

Institutional Abbreviation—**OU**, Geology Museum, University of Otago, Dunedin, New Zealand.

Cladistic Analysis

Data Set—Because of our interest in the interpretation of phylogeny of fossil lineages through morphology, we used the morphological partition of a published matrix (Geisler et al., 2012). The matrix, available in Supplementary Data, includes 311 characters scored for 51 taxa: 21 living and 30 extinct fossil species. Of these characters, 172 could be scored for *Papahu taitapu*. Mysticetes, and unnamed taxa (namely, Charleston Museum specimens reported by Geisler et al., 2012), were removed from the analysis because they were irrelevant (Mysticeti) or included features that cannot be verified from published descriptions (Charleston Museum specimens). All the characters listed by Geisler et al. (2012) are included in the matrix supplied (Supplementary Data) to preserve the relationship with the published list. The matrix presented here includes 29 uninformative characters that are retained to preserve compatibility with the original matrix of Geisler et al. (2012).

Search Methods—Two search strategies were implemented: (1) A non-additive and equally weighted heuristic parsimony analysis of 10,000 replicates was performed using the 'traditional search option' of TNT 1.1 (Goloboff et al., 2008). All characters were treated as non-additive (unordered) and equally weighted (one step). The swapping algorithm used was tree bisection reconnection (TBR); with 10 trees saved per replication. To measure node stability, we used the decay index (Bremer, 1994) and frequency differences (GC) arising from symmetric resampling (Goloboff et al., 2003) based on 2,000 replicates. (2) The second heuristic parsimony analysis was performed using the same parameters above, except that the characters were analyzed using implied weighting (Goloboff, 1993) with the default concavity constant (k = 3). Branch support was reported as frequency differences (GC) arising from symmetric resampling (Goloboff et al., 2003) based on 2,000 replicates.

Review and Changes to Character Scorings—During the character optimization, the scorings of characters recognized as apomorphies of *Papahu taitapu* and closely related taxa were evaluated. Eleven of the original scorings (of Geisler et al., 2012) for *Waipatia maerewhenua* and *Prosqualodon davidis* were modified and seven new scorings (characters 305–311) were added for *Waipatia maerewhenua* (Supplementary Data). Observations were made using the actual type specimen of *W. maerewhenua* (OU 22095), and a replica and high-resolution images of Flynn's (1948) plates of *P. davidis* from the Australian Museum, Sydney. We did not perform an exhaustive assessment of all the character scorings for any given taxon, apart from the one described here.

GEOLOGIC CONTEXT

Specimen OU 22066 was collected in 1987 by R. Ewan Fordyce and Andrew Grebneff 1 km south of Sandhills Creek, North West Nelson (Fig. 1) from pale gray glauconitic siltstone of the Kaipuke Siltstone, of Waitakian to Otaian (Aquitanian to middle Burdigalian) age (Bishop, 1968). The skull was exposed ventral-up on a rock platform at high-tide level; some ventral structures (see Description) were planed off by erosion. The Kaipuke Siltstone and its lateral equivalent, the Tarakohe Mudstone Formation, conformably overlie the Takaka Limestone (Nathan et al., 1986). The collection information (M25/f57 and other localities in Fig. 1) is available from the New Zealand Fossil Record File Database (www.fred.org.nz).

The Kaipuke Siltstone is about 80 m thick (Bishop, 1968) and is exposed along the coast from about 2.5 km southwest of the Paturau River mouth to the Kaipuke Cliffs, 1.5 km southwest of the Anatori River mouth (Fig. 1). It contains a diverse fossil fauna, most notably bryozoans (Bishop, 1968; Gordon et al., 1994) and sparse macroinvertebrates. Matrix from the skull of OU 22066 yielded poorly preserved foraminiferans, but another sample (M25/f59) collected about 100 m north-northeast along strike contained abundant and better-preserved foraminiferans

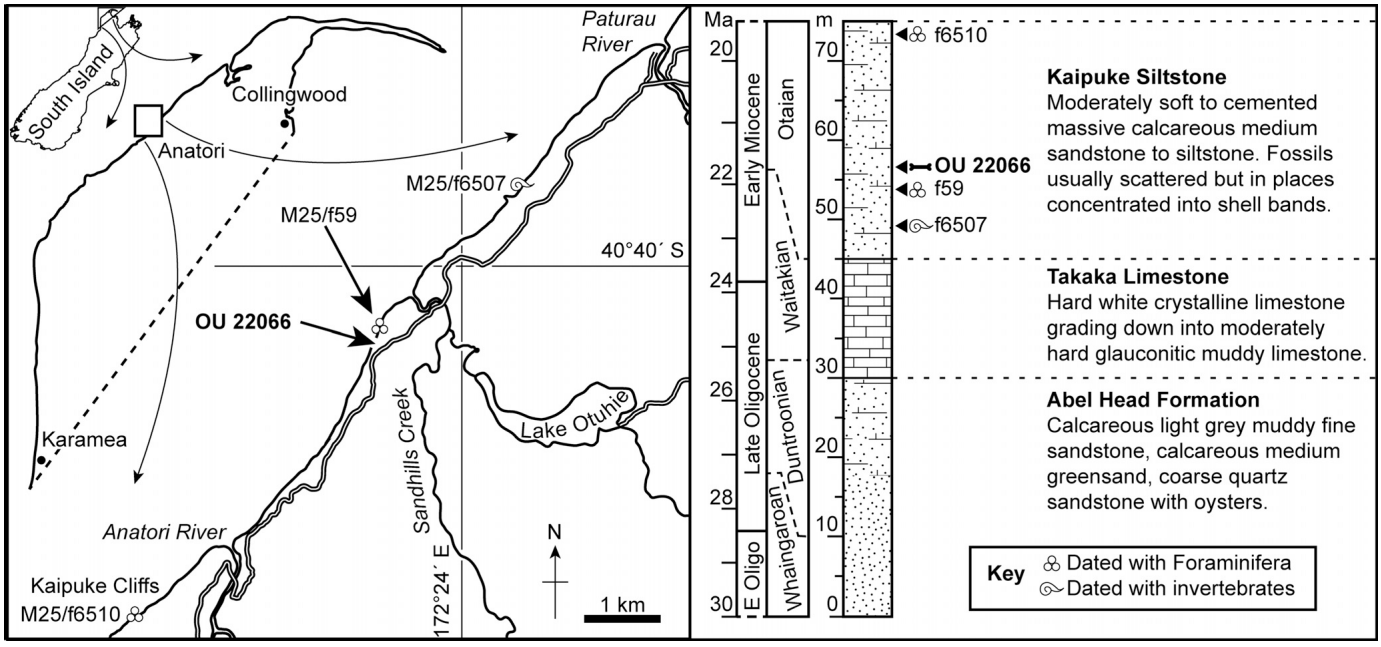

FIGURE 1. Locality map (northwest of the South Island of New Zealand) and stratigraphic section. Dated sample numbers refer to the Fossil Record Electronic Database (www.fred.org.nz). Stratigraphic information summarized from Bishop (1968), Wellman et al. (1981), and Nathan et al. (1986) and information from the New Zealand Fossil Record Electronic Database.

(see Fig. 1), including the index species *Globigerina woodi connecta*, indicating an age of upper Waitakian to Otaian (23–19 Ma, Aquitanian to middle Burdigalian). Based on the foraminiferal abundances (Nathan et al., 1986) and the bryozoan fauna (Gordon et al., 1994), the depositional environment of the Kaipuke Siltstone has been interpreted as a mid-shelf setting with a seasonal temperature range of about 12–17°C. The lithology, massive siltstone suggests deposition below normal storm wave base.

SYSTEMATIC PALEONTOLOGY

CETACEA Brisson, 1762
ODONTOCETI Flower, 1867
Incertae familiae
PAPAHU TAITAPU, gen. et sp. nov.
(Figs. 2–7, Tables 1–3)

Kentriodontidae, Fordyce, 1991:1261.

Holotype—OU 22066, an incomplete skull (lacking part of the rostrum), the left periotic, the right mandible, five vertebrae, and a single rib.

Locality and Horizon—Near Hansen Creek (40.68°S, 172.39°E), 1 km south of the mouth of Sandhills Creek, Northwest Nelson, New Zealand (Fig. 1). Kaipuke Formation. For geological maps, see Bishop (1968) and Rattenbury et al. (1998).

Age—Otaian (21.7–18.7 Ma), in the range middle Aquitanian to middle Burdigalian, early Miocene (correlations from Cooper, 2004; Hollis et al., 2010).

Diagnosis—*Papahu taitapu* is a generalized, medium size odontocete, with 'archaic' features including open mesorostral canal, nares partially roofed by nasals, transversely reduced intertemporal region, well-developed infratemporal crest, and pterygoid sinus complex that does not invade the orbit and temporal fossa. *Papahu taitapu* differs from Xenorophidae in the presence of homodonty, reduced intertemporal constriction, and lacrimal not greatly enlarged; from Agorophiidae in the presence of homodonty and a reduced intertemporal constriction; from Physeteridae and Kogiidae by lacking a wide supracranial basin, pronounced cranial asymmetry, enlarged accessory ossicle on the periotic, and enlarged posterior process of tympanic bulla; from Ziphiidae by the absence of hypertrophied pterygoid sinus fossae, enlarged accessory ossicle on the periotic, and enlarged posterior process of tympanic bulla; from Waipatiidae by lacking double-rooted teeth, nodular nasals, and subcircular periotic fossa, and the apex of premaxilla does not extend posterior to nasals; from Prosqualodontidae and Squalodontidae by the smaller size and the absence of double-rooted teeth, it differs further from Prosqualodontidae in the absence of a deep antorbital notch; from Squalodelphinidae by not having the thick supraorbital process of the frontal and lacking a square-shaped pars cochlearis of the periotic; from Allodelphinidae by lacking

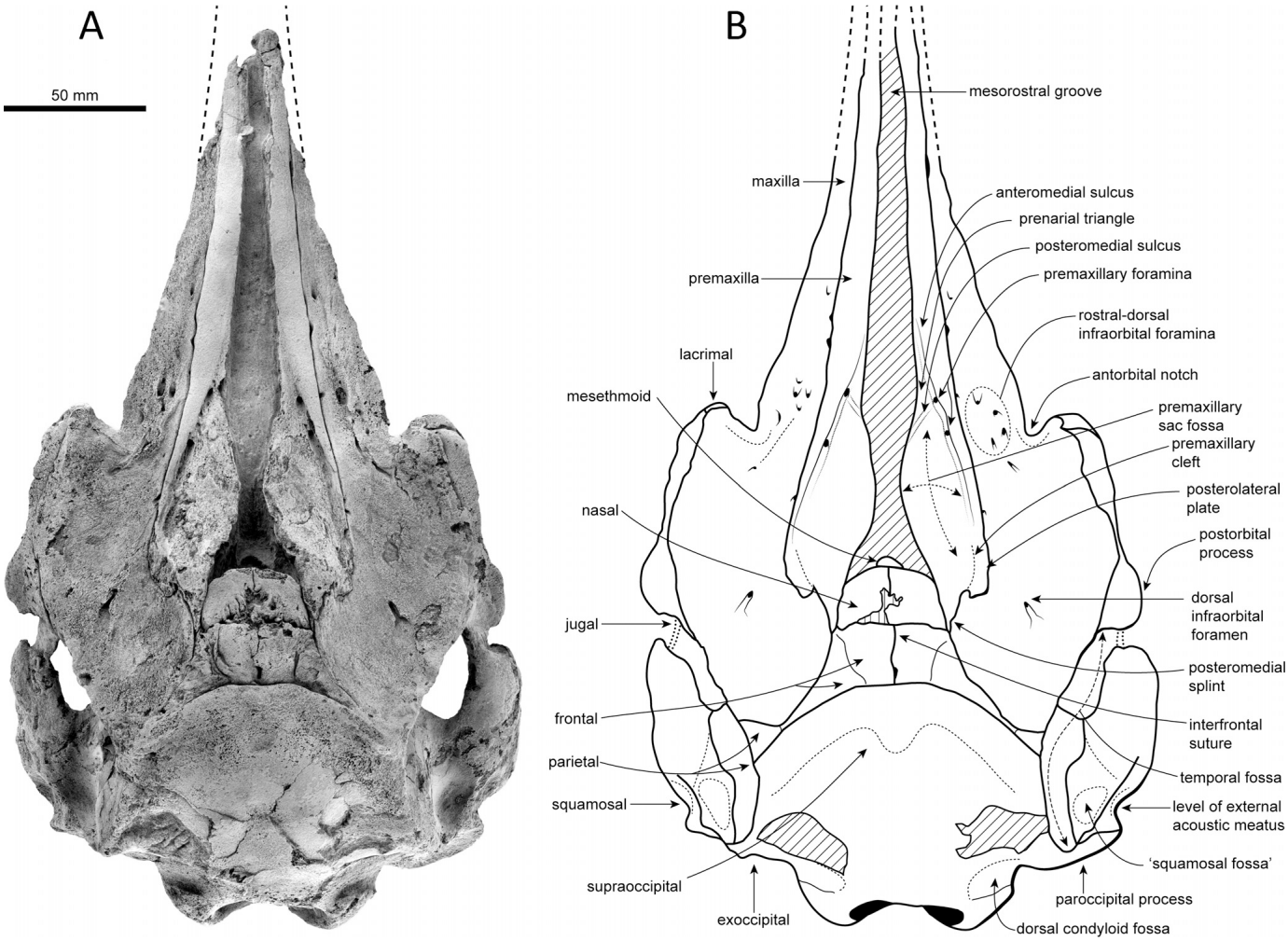

FIGURE 2. *Papahu taitapu*, holotype, OU 22066. **A**, photograph of skull in dorsal view, coated with sublimed ammonium chloride; **B**, line drawing based on **A**. Diagonal hatching indicates areas covered by matrix, vertical hatching indicates poorly preserved areas.

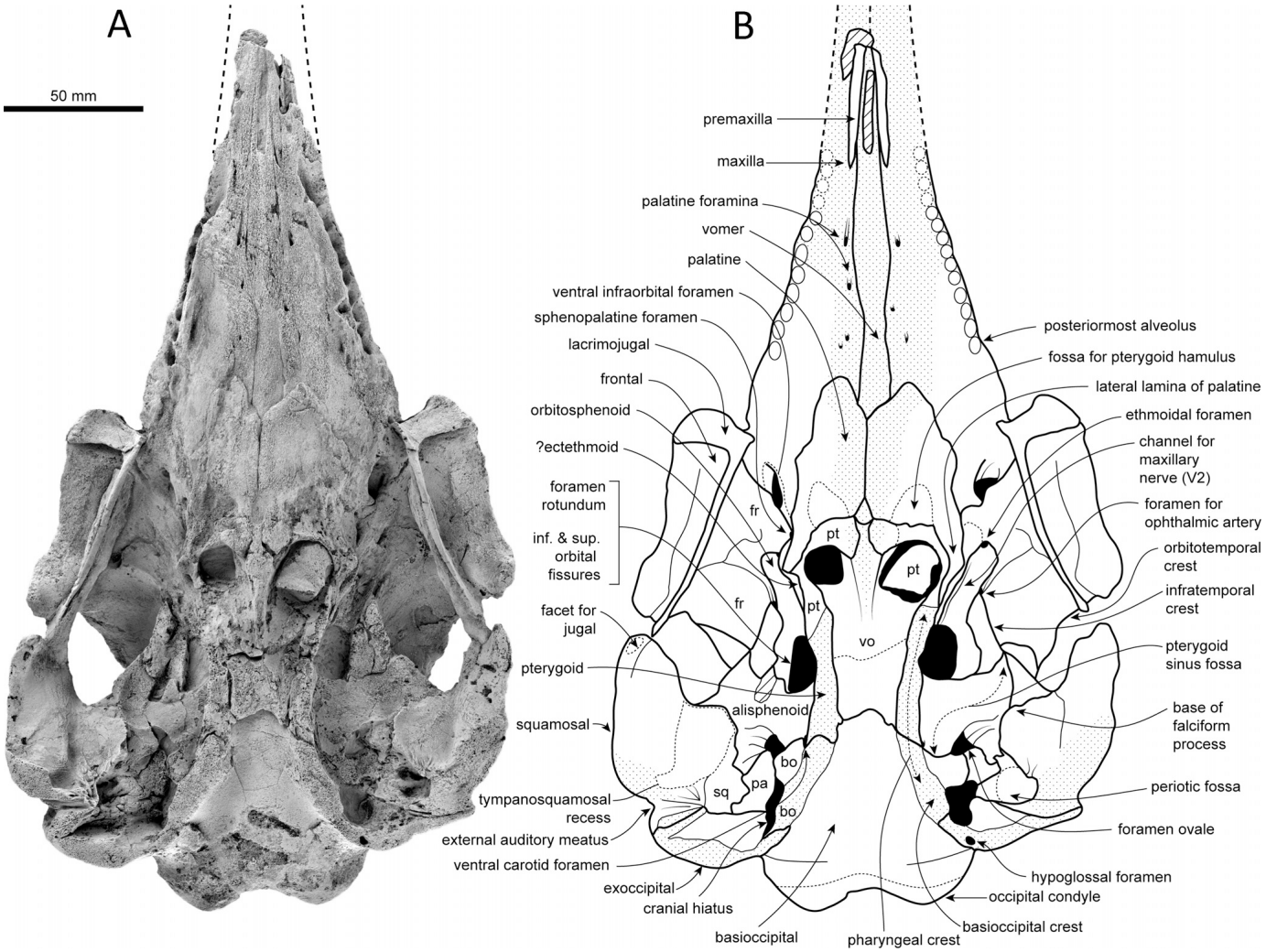

FIGURE 3. *Papahu taitapu*, holotype, OU 22066. **A**, photograph of skull in ventral view, coated with sublimed ammonium chloride; **B**, line drawing based on **A**. Diagonal hatching indicates areas covered by matrix, stippling indicates areas of erosion. **Abbreviations**: **bo**, basioccipital; **fr**, frontal; **pa**, parietal; **pt**, pterygoid; **sq**, squamosal; **vo**, vomer.

elongated nasals, a vertical supraoccipital, and thin, narrow, feathered proximal ends on premaxillae; and from Delphinida by the lack of the parabullary ridge on the periotic and the lack of orbital extensions of the pterygoid sinus. The Dalpiazinidae are too poorly known to be compared in this diagnosis; many of the features used to diagnose dalpiazinids are not preserved in *Papahu taitapu*.

Etymology—Genus: from Pāpahu, a Māori noun for dolphin. If separated, Pā: to close off an open space; Pahū: to burst, explode; in reference to the blow, or the action produced when a cetacean breathes. Species: from Te Tai Tapu, Māori location use for the northwest coast of the South Island of New Zealand. Te: the; Tai: tide or coast; tapu: special, sacred. Pronounciation: paa-pa-hu tai-ta-pu, with a long first a, the a pronounced as in English 'far', u as in 'put' in both instances.

DESCRIPTION

Skull

The skull (Figs. 2–5, Table 1) is low and mostly symmetrical. The incomplete, broad-based rostrum preserves a distinctive open mesorostral canal and a slight degree of directional asymmetry in the antorbital notches (the left notch is more open and less 'V'-shaped than the right one). The posterior 75 mm of the rostrum preserve natural margins with a broad triangular profile that tapers forwards (Figs. 2, 3). Each premaxillary sac fossa projects onto the rostrum. The alveoli indicate only single-rooted teeth and homodonty is inferred, but no teeth are preserved. The vertex is tabular, with plate-like nasals that overhang the nares, partly obscuring them in dorsal view (Fig. 2; the nares are infilled with matrix). Each open temporal fossa fully reveals the squamosal in dorsal view. The infratemporal crest restricts the pterygoid sinus complex to the basicranium. The pterygoid sinus fossa occupies all of the pterygoid bone and probably extends into the posterior margin of the palatine (Figs. 3, 4). The cranium is moderately compressed dorsoventrally by burial compaction, with a transverse fracture plane that runs dorsal to the occipital condyles, and along the supraoccipital-parietal suture of both temporal fossae. The dorsoventral compression is more accentuated on the left, with the left orbit located more ventrally, producing differential exposure of the temporal fossa in ventral view and also affecting exposure of the palatines. The skull was retrodeformed in lateral view by eye, by accommodating the depth of the posterior portion of the mandible and using the positions of the

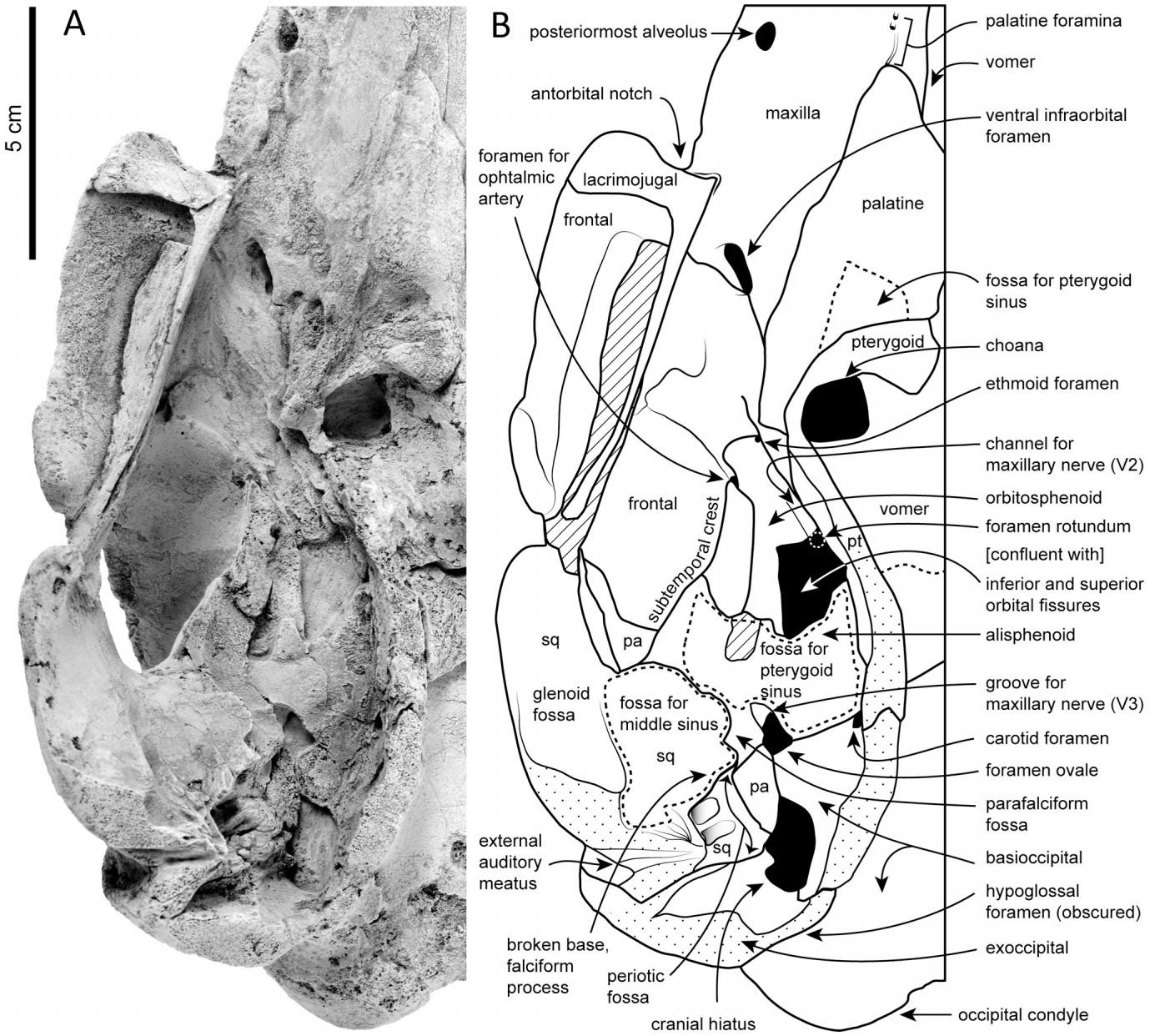

FIGURE 4. *Papahu taitapu*, holotype, OU 22066. Oblique ventral view of the basicranium. **A**, photograph, specimen coated with sublimed ammonium chloride; **B**, line drawing based on **A**. Diagonal hatching indicates areas covered by matrix, stippling indicates areas of erosion. **Abbreviations**: **pa**, parietal; **pt**, pterygoid; **sq**, squamosal.

squamosal and the lacrimojugal relative to the postorbital process of the frontal (Fig. 5E).

Premaxilla—Each premaxilla extends medially from the apex of the preserved rostrum to the cranial vertex. In dorsal view (Fig. 2), the premaxilla is smooth-surfaced, relatively linear and narrow, bordering a wide matrix-filled mesorostral canal (Fig. 2, Table 1). The canal is widest at the level of the anterior premaxillary foramen, rapidly narrowing posteriorly to reach the narrowest part at the midpoint of the premaxillary fossa. At the vertex, the posterior part of the premaxilla extends posteriorly and forms a posteromedial splint that inserts between the maxilla and the nasal, contacting the frontal with its very narrow, pointed posterior end. A short premaxillary cleft extends forward from where the premaxilla separates into the posteromedial splint and the posterolateral plate. In lateral view (Fig. 5C), the posterolateral plate of the premaxilla is clearly distinct and extends posteriorly from the posterolateral sulcus of the premaxilla to a level 7–8 mm posterior to the anterior edge of the nasals. On the rostrum, the premaxilla is parallel-sided, slightly convex transversely and elevated above the maxilla, but flattens posteriorly as it widens towards the base of the rostrum. Dorsally (Fig. 2), there is a pair of bilaterally asymmetrical foramina on each premaxilla (separated from each other by 20 mm on the left and 13 mm on the right). The anterior premaxillary foramen opens about 10 mm anterior to the antorbital notch, associated with two sulci best seen on the right. A short anteromedial sulcus arises

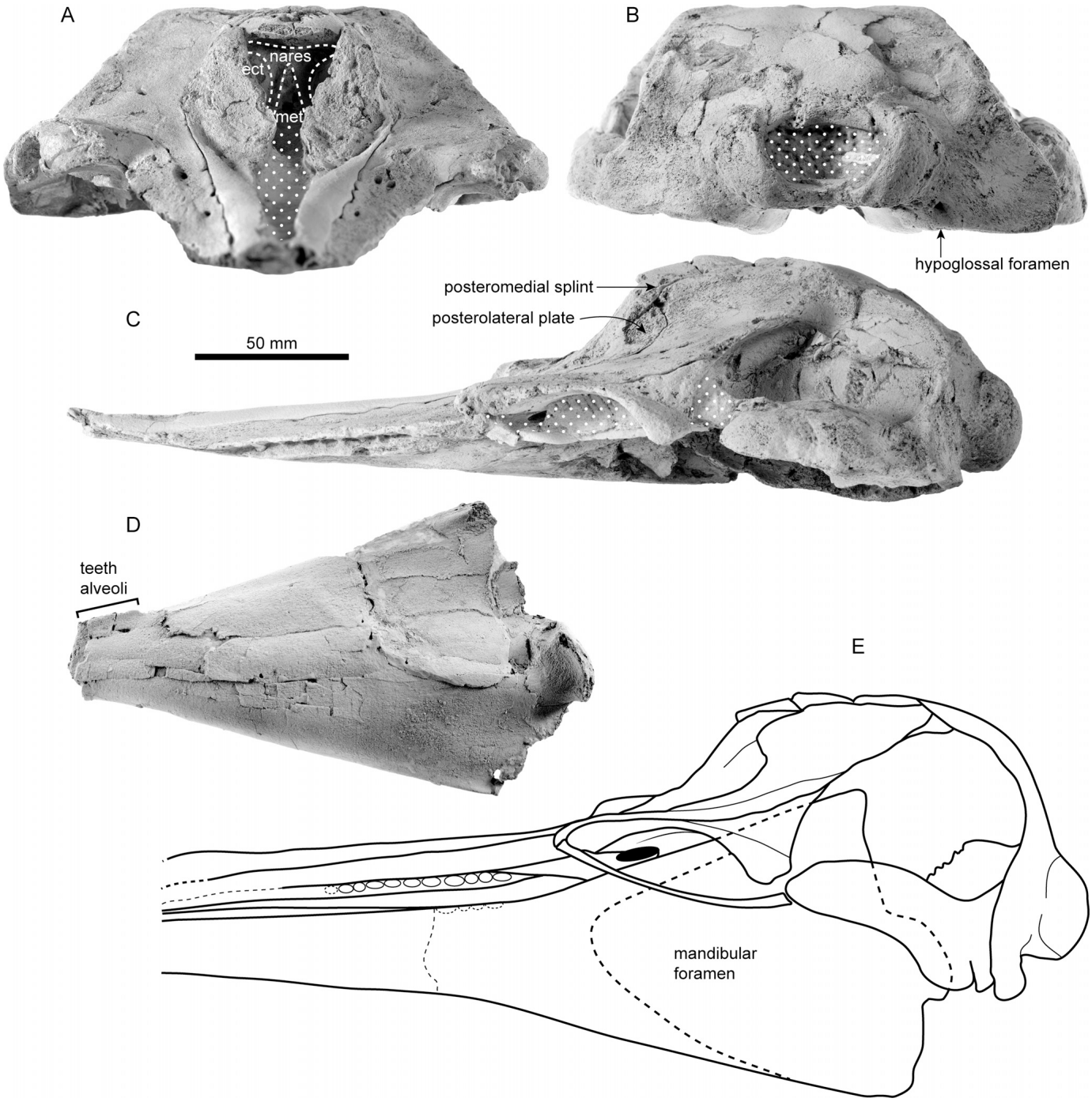

FIGURE 5. *Papahu taitapu*, holotype, OU 22066. Photographs of the skull, coated with sublimed ammonium chloride. **A**, anterior view; **B**, posterior view; **C**, lateral view; **D**, photograph of right mandible in lateral view, reflected to appear on left view of skull; **E**, line drawing of retrodeformed skull based on **C** and **D**. **Abbreviations**: **ect**, ectethmoid; **met**, mesethmoid.

at the foramen, to become indistinct as it passes forward into a long, narrow, depressed medial part of the premaxilla—the prenarial triangle—which is the fossa for the nasal plug muscle (the equivalent surface is less well preserved on the left). The posteromedial sulcus also arises at the premaxillary foramen; the sulcus is an indistinct short, shallow groove, apparent on the right in raking light or by palpation, and directed posteriorly at about 45 degrees towards the mesorostral canal. The posteromedial sulcus separates the premaxillary sac fossa posteriorly from the nasal plug muscle fossa anteriorly. The slightly concave premaxillary sac fossa is rough-surfaced anteriorly, and smoother posteriorly. The posterior premaxillary foramen opens level with the base of the rostrum and passes into a posterolateral sulcus that runs along the prominently raised, smooth-surfaced, elongate lateral border of the premaxilla, also forming the lateral border of the premaxillary sac fossa.

TABLE 1. Skull and mandible measurements (in mm) of *Papahu taitapu*, gen. et sp. nov., OU 22066.

Condylobasal length	+ 321
Length of rostrum	+ 144
Width of rostrum at base (anterior to antorbital notches)	94
Width of premaxillae at base of rostrum	52
Greatest width of mesorostral canal	20
Length of the left orbit	53
Width across preorbital processes of frontals	151
Width across postorbital processes of frontals	178
Maximum width of left premaxillary sac fossa	17
Bizygomatic width	182
Maximum length of left squamosal	61
Greatest width of bony nares (near anterior edge of nasals)	32
Greatest width across nasals	36
Width across occipital condyles	75
Number of maxillary teeth alveoli—left row	+ 10
Number of maxillary teeth alveoli—right row	+ 8
Diameter of posterior-most alveolus in maxilla (left)	5
Distance from antorbital notch to posterior-most alveolus (left)	27
Height of mandible	98

+, incomplete.

Maxilla—In dorsal view (Fig. 2), the rostral part of the maxilla is clearly separated from the premaxilla by an unfused suture. The maxilla is relatively thin and wide along the rostrum, with a pronounced dorsal exposure at the rostral base (Table 1). The antorbital notch is formed by the maxilla, but the lateral half of the right antorbital process exposes the lacrimojugal anteriorly and the frontal laterally. The numerous dorsal infraorbital foramina on the maxilla vary bilaterally in position and number (five on the left, seven on the right), with some of them located at the premaxilla-maxilla suture. The anterior-most dorsal infraorbital foramen opens about 50 mm anterior to the base of the rostrum, whereas the posterior-most foramen is in line with the postorbital process of the frontal, at the center of the ascending process. At the orbit, the maxilla does not fully cover the frontal in dorsal view. The outer margin of the maxilla is roughly straight from the postorbital process back over the temporal fossa. At the vertex, the maxilla contacts the thin posterolateral splint of the premaxilla and the frontal without contacting the nasal. The rounded posterior margin of the maxilla is separated from the supraoccipital by a thin strip of frontal.

In ventral view (Fig. 3), all the preserved tooth alveoli (10 on the left, eight on the right) are located in the maxilla, and all appear to be single-rooted. The posterior-most alveolus is about 26 mm anterior to the antorbital notch. The rostrum is mainly formed by the maxilla, but the premaxilla and the vomer are exposed anteriorly. Natural exposure is limited because of erosion of the ventral surface (see stippling, Fig. 3B), but some original surface is preserved posteriorly, near the contact with the palatines. Medial to the antorbital notch, the zygomatic recess of the maxilla receives the lacrimojugal. The posterior-most part of the maxilla differs slightly in its contribution to the left and right ventral infraorbital foramina, forming the medial and anterolateral borders on the left and almost completely enclosing the right foramen (Figs. 3, 4).

Vomer—In dorsal view (Fig. 2), the vomer is obscured by matrix that could not be removed easily. The mesorostral canal is widely open, reaching a maximum width of 21 mm near the anterior premaxillary foramen. In ventral view (Fig. 3), the incomplete, partially eroded vomer is exposed on the rostrum, separating the premaxillae along the anterior third of the preserved rostrum and the maxillae on the posterior two-thirds of the rostrum. The vomer is exposed between the posterior portion of the palatines and the pterygoids and then continues as a vomerine crest that divides the choanae (Fig. 3). Posteriorly, the vomer covers the basioccipital to the level of the foramen ovale and contacts the medial lamina of the pterygoid laterally.

Lacrimojugal—Both lacrimojugal bones are more or less complete (Figs. 3–5), with the lacrimal and jugal fused without evident suture. In ventral view, the anterior part of the lacrimal is transversely wide (~27 mm) and forms the convex ventral margin of the antorbital notch (Figs. 3, 4). Laterally, the lacrimal underlies the frontal and is prolonged forward to contribute to a rounded (right) or triangular (left) antorbital notch. The lateral border is oblique, whereas the posterior border is slightly concave. Ventrally, there are prominent open sutures with the frontal and maxilla, and the lacrimojugal does not extend toward the ventral infraorbital foramen. The jugal arises at the inner margin anteriorly; it is slender, rod-like, compressed laterally, and about 83 mm long. Originally, the styliform portion of the jugal would have been more arched, with its posterior end contacting the ventral apex of the zygomatic process of the squamosal (where a remnant suture is preserved on the left squamosal). The position and shape of each jugal suggests that the matching zygomatic process of the squamosal is not too far displaced from its original position (the squamosal has been slightly displaced posterodorsally; see Fig. 5C, E).

Ethmoid—The configuration of the external bony nares (Fig. 5A) resembles that of other archaic odontocetes, particularly '*Squalodon*' *crassus* as shown by Kellogg (1928:fig. 22) and undescribed 'dalpiazinids' from New Zealand (such as OU 22397). The wide mesethmoid (up to 13 mm wide) forms the most dorsal partition of the narial passages, and posteriorly divides the laterally compressed olfactory foramina. Laterally, the ectethmoids form the external surfaces of these foramina, the exact limits of the ethmoid bones are not known; the area is poorly preserved and attempts to prepare it were unsuccessful.

Nasal—The symmetrical plate-like nasals partially roof the vertically directed nares at the tabular vertex of the skull. The thin anterior border of each nasal becomes thicker posteriorly. The posterior border of each nasal is in line with the postorbital process of the frontal (Fig. 2). Each plate-shaped nasal is slightly convex on both the dorsal and ventral faces, and slightly depressed dorsally along the midline (Fig. 5A, C, E). Each nasal contacts the ascending process of the premaxilla laterally and the frontal posteriorly. The internasal suture is clearly defined anteriorly, but becomes irregular and deepens slightly posteriorly, creating a natural fissured triangular basin (Fig. 2).

Frontal—In dorsal view, each frontal is almost completely covered by the maxilla (Fig. 2), with only a thin strip of frontal separating the maxilla from the supraoccipital. At the vertex, the frontals are slightly convex anteromedially (with the left frontal more domed than the right one) and flat posterolaterally (Fig. 5C, E). The interfrontal suture is fused posteriorly, but remains visible anteriorly. The dorsal exposure of the frontal widens posteriorly from the contact with the nasals, passing into the thin strip that surrounds the posterior edges of the maxillae. The antorbital and the postorbital processes of the frontal are relatively thin dorsoventrally, with the antorbital process wedging in between the maxilla and the lacrimojugal. The apex of the postorbital process has a small indentation, which probably marks its proximity to the zygomatic process of the squamosal. In ventral view (Figs. 3, 4), the antorbital process of the frontal is covered by the lacrimojugal. The wide orbit passes back medially into a posteriorly elongate shallow groove on the supraorbital process leading to the foramina of the orbit. Medially, the well-developed ventral orbital crest runs obliquely to form the lateral edge of the infraorbital foramen. The ethmoidal foramen marks the frontal-orbitosphenoid suture. The anterior end of the conspicuous infratemporal crest has a prominent foramen, here interpreted as the foramen for the ophthalmic artery (see Fordyce, 2002:fig. 13). The frontal is exposed in the temporal fossa, where it contacts the parietal.

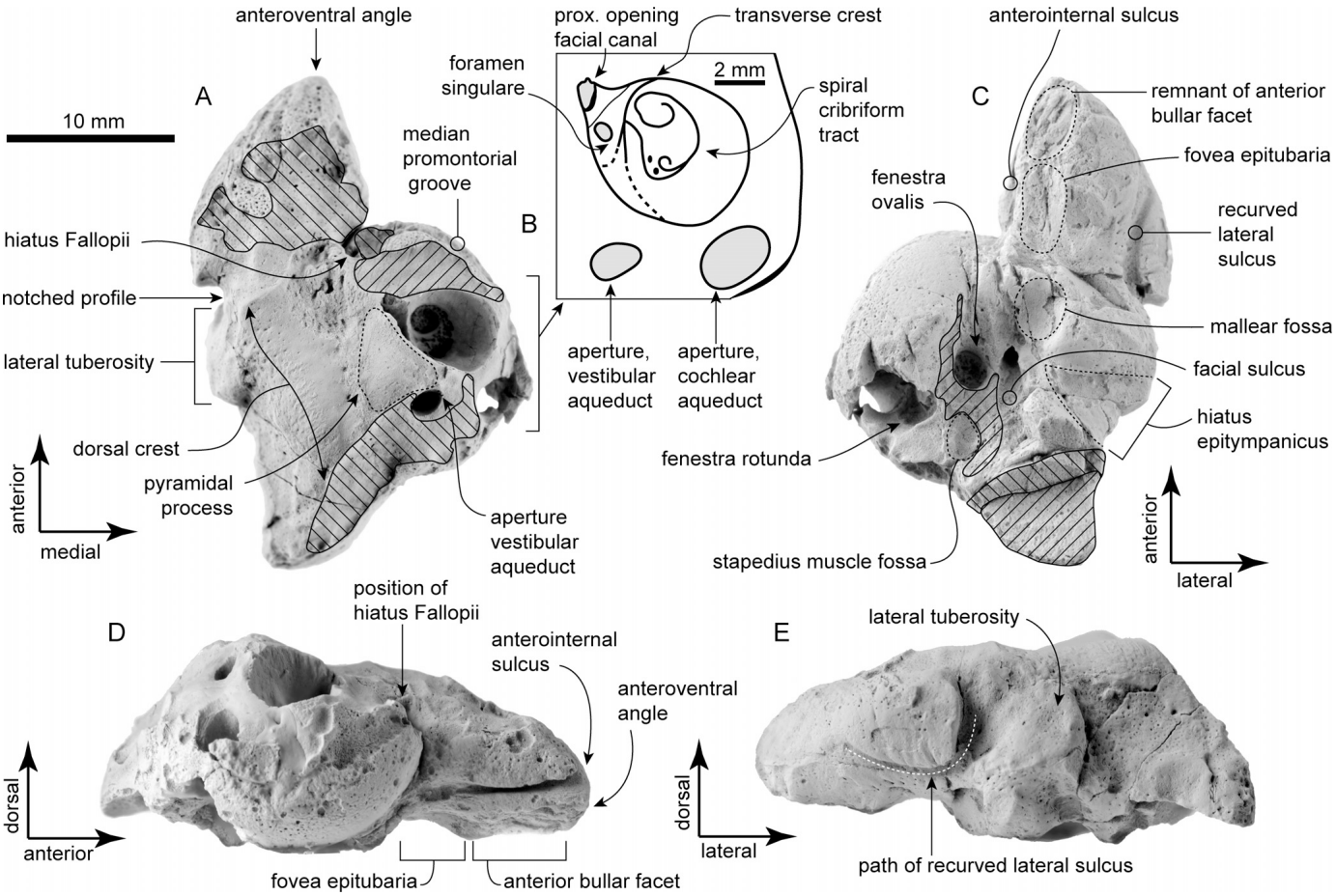

FIGURE 6. *Papahu taitapu*, holotype, OU 22066. **A**, photograph of left periotic in cerebral (dorsal) view; **B**, camera lucida sketch of the pars cochlearis in dorsal view; **C**, photograph of left periotic in ventral view, coated with sublimed ammonium chloride; **D**, photograph of left periotic in medial view, coated with sublimed ammonium chloride; **E**, photograph of left periotic in lateral view, coated with sublimed ammonium chloride. Diagonal hatching indicates damaged areas; the different directions of hatching aim to aid a sense of perspective.

Supraoccipital, Exoccipital, and Basioccipital—The supraoccipital is greatly exposed in dorsal view (Fig. 2). The nuchal crest is not elevated over the vertex, and is low and smooth. The anterior contact with the frontal is curved and regular.

The occipital condyles have probably retained their original width (maximum condylar width is 75 mm) despite some compression and deformation of the cranium (Figs. 2, 4B). Both ventral and dorsal condyloid fossae are present but not very marked. In ventral view (Fig. 3), the exoccipital can be located posterior to the squamosal and parietal, forming the posterolateral edge of the cranial hiatus and descending into a crest that is continuous with the basioccipital crest (Fig. 3). Here, erosion has exposed the hypoglossal foramen on the left exoccipital and obliterated any jugular notch, leaving the paroccipital process mostly eroded.

The contact of the basioccipital and basisphenoid is not visible. Posterior to the vomer, the basioccipital extends posteriorly for about 66 mm. The basioccipital crests are eroded ventrally. The suture between the basioccipital crest and the medial lamina of the pterygoid is level with the ventral carotid foramen, which is in turn level with the broken base of the falciform process.

Parietal—In dorsal view (Fig. 2), a few millimeters of the parietal is exposed forming the corner of the intertemporal constriction at the junction of the nuchal and orbitotemporal crests. The parietal forms the anterior medial wall of the temporal fossa, extending anteroventrally to form the anterior half of the infratemporal crest. The presence of an interparietal cannot be confidently stated despite two different periosteal textures being apparent on the supraoccipital shield: a rugose band that starts at the nuchal crest (for the rhomboideus capitis?), and a relatively smooth surface that surrounds the area dorsal to the foramen magnum. Ventrally, the parietal is exposed in the periotic fossa, forming a plate medial to the squamosal that contacts

TABLE 2. Periotic measurements (in mm) of *Papahu taitapu*, gen. et sp. nov., OU 22066.

Maximum anteroposterior length	+30.6
Length anterior process (apex anterior process to anteromedial pars cochlearis)	10.6
Maximum width of anterior process at base	11
Maximum length acoustic meatus (anterior limit facial canal to posterior rim)	6.5
Maximum width of acoustic meatus (ventral limit facial canal to medial rim)	7.2
Width of posterior process at base, perpendicular to anteroposterior axis	9
Maximum length of pars cochlearis (anteroposterior length)	12.3
Maximum transverse width of pars cochlearis (internal edge to fenestra ovalis)	10.6

+, incomplete.

the basioccipital to separate the foramen ovale from the cranial hiatus (Figs. 3, 4).

Squamosal—The squamosal is well exposed in dorsal view, not roofed by the frontal and the ascending process of the maxilla (Fig. 2). The preserved positions of both zygomatic processes of the squamosal are unevenly distorted by burial compression, resulting in greater ventral erosion of the left squamosal (Fig. 3). The natural position was probably more anterior (anterior tip of squamosal in line with nasofrontal suture) and ventral, closer to the postorbital process of the frontal (Fig. 5E). The anterior face of the zygomatic process of the squamosal has two facets: a short dorsal part that originally approximated the postorbital process of the frontal; and a slightly prolonged, slender ventral part that helps to form the zygomatic arch in conjunction with the jugal. The zygomatic process of the squamosal has a transversely convex (curved) dorsal surface and is relatively robust. Posteriorly, dorsal to the external auditory meatus (preserved only on the right side), the zygomatic process develops a small fossa that serves as the origin for some or all of the sternomastoideus, scalenus ventralis, longus capitis, and mastohumeralis muscles (Fordyce, 1994). In line with this fossa, but on the temporal surface of the squamosal, another well-developed fossa is present, referred to as the 'squamosal fossa' by Barnes (1985) and Geisler and Sanders (2003). The temporal plate of the squamosal overlies the parietal and contacts the exoccipital posteriorly, forming an incipient temporal crest. In lateral view (Fig. 5C, E), the zygomatic process of the squamosal increases in height posteriorly, but it is eroded ventrally to an unknown extent. Both of the postglenoid processes are eroded, but the right one is more complete, with the postglenoid notch still visible. The right postglenoid process is relatively wide and anteroposteriorly thin, with a prominently excavated tympanosquamosal recess for the middle sinus. In ventral view (Figs. 3, 4), between the zygomatic and the falciform processes, a smooth large fossa forms the anterior part of the incomplete tympanosquamosal recess. The broken base of each falciform process is preserved roughly in level with the foramen ovale. Further posteriorly, a low crest (pristine on the right) separates the tympanosquamosal recess from the periotic fossa (Fig. 4). The periotic fossa appears dorsomedial to the spiny process. With the periotic in place, the supratrabecular ridge (sensu Fordyce, 1994) contacts the remnant of the dorsal crest of the periotic, and the fossa opens laterally and dorsally. In this case, the two parts of the periotic fossa are anteroposteriorly compressed and form slit-like structures with many foramina. A sulcus leads anteromedially from the periotic fossa to the foramen ovale.

Pterygoid and Pterygoid Sinus Fossae—In ventral view (Figs. 3, 4), the eroded pterygoid bone can be traced anteriorly to the prominent posterior depression of the palatine, where some fragments remain in place and form the anterolateral wall of the choana. The thin bone-overlying matrix in the left choana is interpreted as a fragment of pterygoid from the left hamulus, and the surface visible in ventral view is probably the ventral face of the more-dorsal or choanal lamina of the hamulus. The surface of the pterygoid fragment carries ridges similar to those on the comparable hamular surface of the living *Lagenorhynchus obscurus*. The medial lamina of the pterygoid forms most of the lateral wall of the choana and, passing back, the pharyngeal crest; the medial lamina contacts the basioccipital on the crest slightly anterior to the ventral carotid foramen of the basisphenoid. The components of the pterygoid air sinus complex that have bony structures preserved are the fossa for the pterygoid sinus (sensu stricto) that occupies a significant smooth, shallow, and obliquely elongated excavation on the alisphenoid (22 mm wide and 29 mm long), the depression on the palatines, anterior to the choanae, and the tympanosquamosal recess for the middle sinus (Fig. 4). No fossae for parts of the pterygoid sinus are present in the orbit, and it is unlikely that the sinus system invaded the orbits, given the presence of a well-defined infratemporal crest and the lack of any obvious path for orbital extension of the pterygoid sinus anterior to the foramen rotundum (Figs. 3, 4). Given the erosion of the posterior part of the basioccipital crest and the paroccipital process, and loss of the tympanic bulla, it is not possible to ascertain the presence or absence of a peribullary sinus fossa.

TABLE 3. Vertebral measurements (in mm) of *Papahu taitapu*, gen. et sp. nov., OU 22066.

Measurement	C2	C3	Lumbar
Maximum height	73	+ 62	+ 93
Maximum width	85	82	+ 85
Height of body	27p	31	47
Width of body	40p	40	52
Length of body	20 + 13 (dens)	13	+ 31
Height of neural arch	29	22	19p

+, incomplete; p, measured from posterior face.

Alisphenoid, Basisphenoid, and Orbitosphenoid—The orbitosphenoid is largely fused to the adjacent bones. It extends from the ethmoidal foramen of the frontal anteriorly to the groove for the optic canal posteriorly.

The anterior limit of the alisphenoid is marked by the foramen rotundum (Fig. 4). Posteriorly, the alisphenoid forms the anterior edge of the foramen ovale, contacting medially the basioccipital and laterally the tympanosquamosal recess of the squamosal posterior to the parafalciform fossa. There is a large fossa for the pterygoid sinus preserved on the alisphenoid. A splint of the alisphenoid extends back along the inner margin of the falciform process. Further anteriorly, the alisphenoid-squamosal suture is present near the groove for the mandibular nerve, but anterolateral limits are uncertain.

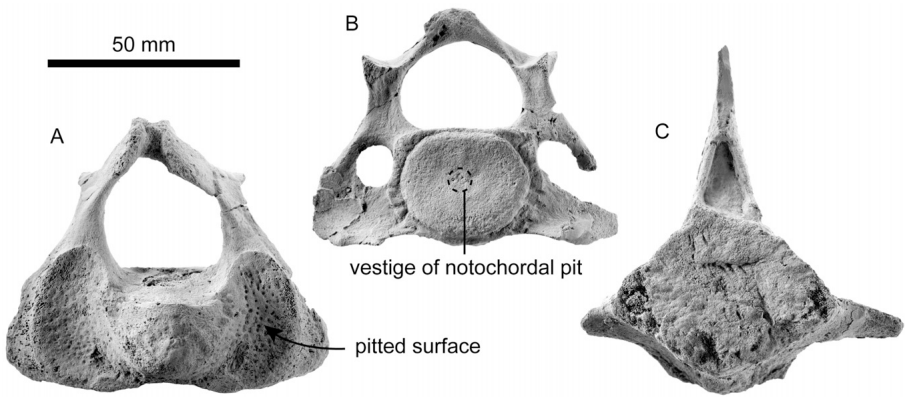

FIGURE 7. *Papahu taitapu*, holotype, OU 22066. **A**, photograph of the axis (C2) in anterior view; **B**, photograph of the third cervical (C3) in anterior view; **C**, photograph of a lumbar vertebra. Fossils coated with sublimed ammonium chloride.

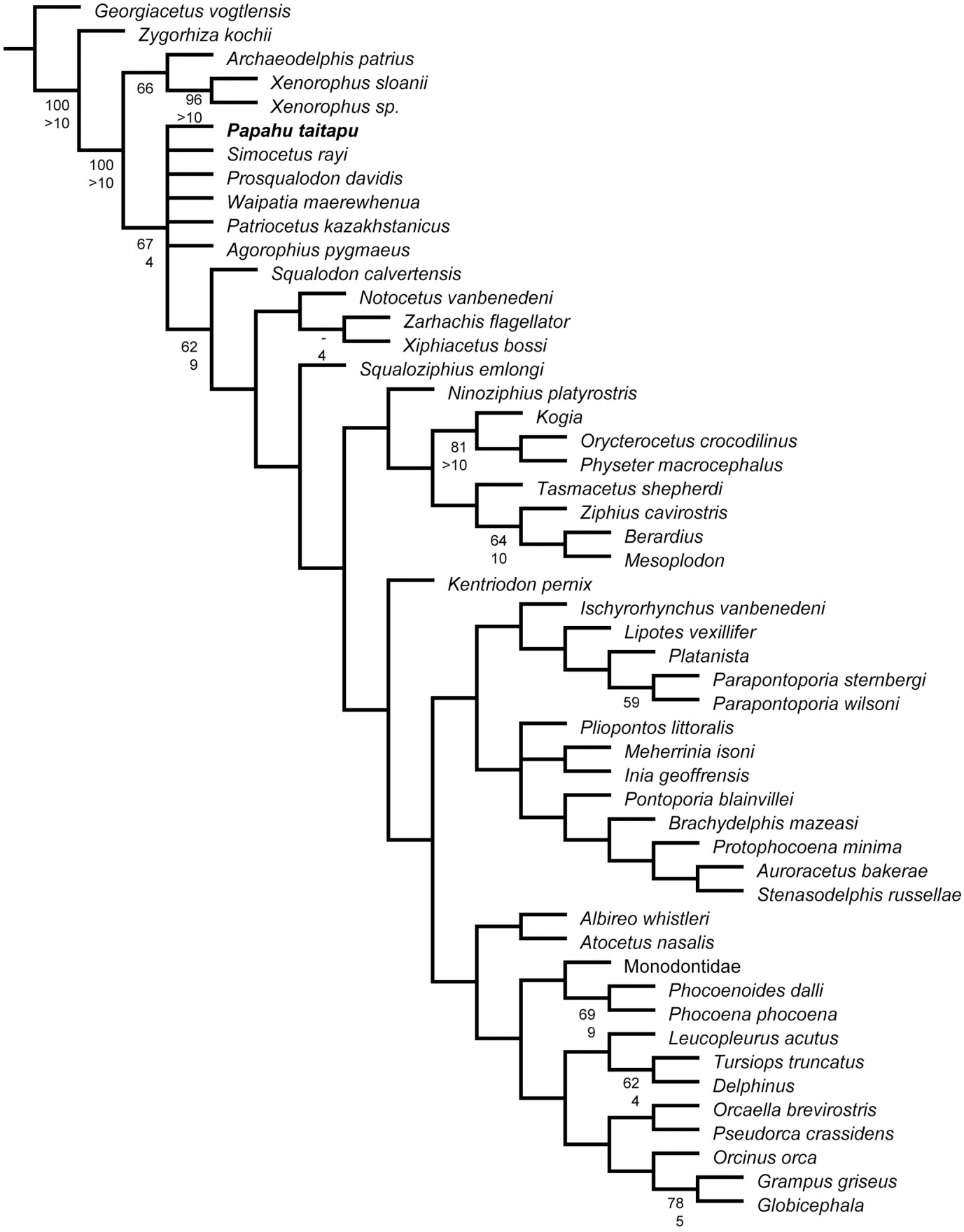
Georgiacetus vogtlensis
Zygorhiza kochii
Archaeodelphis patrius
Xenorophus sloanii
Xenorophus sp.
Papahu taitapu
Simocetus rayi
Prosqualodon davidis
Waipatia maerewhenua
Patriocetus kazakhstanicus
Agorophius pygmaeus
Squalodon calvertensis
Notocetus vanbenedeni
Zarhachis flagellator
Xiphiacetus bossi
Squaloziphius emlongi
Ninoziphius platyrostris
Kogia
Orycterocetus crocodilinus
Physeter macrocephalus
Tasmacetus shepherdi
Ziphius cavirostris
Berardius
Mesoplodon
Kentriodon pernix
Ischyrorhynchus vanbenedeni
Lipotes vexillifer
Platanista
Parapontoporia sternbergi
Parapontoporia wilsoni
Pliopontos littoralis
Meherrinia isoni
Inia geoffrensis
Pontoporia blainvillei
Brachydelphis mazeasi
Protophocoena minima
Auroracetus bakerae
Stenasodelphis russellae
Albireo whistleri
Atocetus nasalis
Monodontidae
Phocoenoides dalli
Phocoena phocoena
Leucopleurus acutus
Tursiops truncatus
Delphinus
Orcaella brevirostris
Pseudorca crassidens
Orcinus orca
Grampus griseus
Globicephala
100
>10
66
96
>10
100
>10
67
4
62
9
-
4
81
>10
64
10
59
69
9
62
4
78
5

Although the basisphenoid is fused to the basioccipital posteriorly, its position is marked by the carotid foramen (Fig. 4). There is a distinctive bilateral depression posterior to the vomer and medial to the carotid foramen; this structure is also seen in *Squaloziphius emlongi* (see Muizon, 1991:fig. 1b).

Palatine—The large palatines (Fig. 3) extend anteriorly beyond the antorbital notch and contact each other along the midline, but are separated by the maxillae and vomer anteromedially. The area of the left palatine looks bigger than the right one in ventral view (Fig. 3), but this effect is caused by a slight degree of asymmetric deformation: the left side of the skull is both more compressed and more laterally exposed (in ventral view, Fig. 3) than the right side. Each palatine is bluntly projected forward, so that the two palatomaxillary sutures have the shape of an inverted 'W.' The ventral face of each palatine passes smoothly up into the thin and indifferently preserved lateral face without any obvious palatal crest. Anterior to the choana, a large posterior depression on each palatine (22 mm long and 22 mm wide) probably held part of the hamular lobe of the pterygoid sinus, with the hamulus sutured around part of the depression; the bone surface is too poorly preserved to be sure of details. There is no sign of the greater palatine foramen, normally associated with the maxillopalatine suture, and the foramen may have been eroded away. Traces of the palatine sulcus remain on the maxilla. We interpret the more obvious foramina well anterior to the preserved apex of the palatine as the lesser palatine foramina.

Periotic—The periotic of *Papahu taitapu* (Fig. 6, Table 2) was preserved a few millimeters from its original position when the skull was excavated. It was damaged inadvertently by acid and air-abrasive during preparation, so that some details are lost (Fig. 6, dashed area). In lateral view, the profile of the periotic is notched and its longitudinal axis is prolonged anteroventrally.

The anterior process is conical and triangular in dorsal view, slightly longer than the body of the periotic (Fig. 6A). With the periotic sitting flat on the dorsal surface (ventral view, Fig. 6C), the anterior process is slightly flattened obliquely (ventrolateral to dorsomedial). The anterodorsal angle is damaged, whereas the anteroventral angle is smooth and poorly defined. The fovea epitubaria for the accessory ossicle is anteroposteriorly elongated (Fig. 6C). A remnant of the anterior bullar facet is present and there is no parabullary ridge. Toward the ventral margin, the lateral face has a prominent recurved sulcus (Fig. 6C, E), but its homology with the oblique anteroexternal sulcus of Archaeoceti and basal Odontoceti and Mysticeti is unclear. The circular mallear fossa is large (~4 mm diameter), with prominent anterior and lateral margins. A lateral tuberosity is present, but is not well developed (Fig. 6E). The anterointernal sulcus can be seen as a prominent linear fissure in ventral and medial views (Fig. 6D).

The pars cochlearis is inflated and longer than the anterior process. In dorsal view, the internal acoustic meatus is subcircular (Fig. 6B). The oval-shaped proximal opening of the facial canal ends in a small notch anteriorly, the hiatus Fallopii (Fig. 6A, D). The hiatus Fallopii opens about 4 mm anterior to the facial canal, near the anterior end of the pars cochlearis; the same structure was identified in *Waipatia maerewhenua* by Fordyce (1994) and in *Eurhinodelphis cocheteuxi* by Lambert (2005) as the foramen for the greater petrosal nerve. A raised, anteroposteriorly oriented transverse crest separates the facial canal and foramen singulare from the spiral cribriform tract (Fig. 6B). The aperture for the cochlear aqueduct is visible in dorsal view and it is oval and bigger than the aperture for the vestibular aqueduct. There is a tubercle between the internal acoustic meatus and the aperture for the vestibular aqueduct that does not appear to be associated with the dorsal crest of the periotic and therefore is identified here as the pyramidal process. In ventral view (Fig. 6C), the pars cochlearis is elongated obliquely posteromedially. The fenestra ovalis is about 2 mm in diameter and opens posteroventrally. There is no evidence of the fossa incudis. The lateral rim of the fenestra rotunda was damaged during preparation.

In dorsal view, the body of the periotic has a poorly developed dorsal crest (Fig. 6A). In ventral view (Fig. 6C), the facial canal opens slightly anterior to the fenestra ovalis; the facial sulcus is directed posterolaterally. Laterally, the epitympanic hiatus extends longitudinally for 3 mm from the edge of the lateral tuberosity to the edge of the posterior process. The shallow and subspherical fossa for the stapedius muscle is located in the posteroventral corner of the pars cochlearis (Fig. 6C); details are lost because of damage.

Mandible—Only the right ramus and about 24 mm (last two or three alveoli) of the body are preserved (Fig. 4D, E, Table 1). All of the mandibular teeth are lost and the alveolar walls are too poorly preserved to count the alveoli or to see their shape. The coronoid process is damaged and the mandibular notch is not identifiable. The coronoid crest is thinnest (less than 1 mm) posteriorly.

In dorsal view, the posterior part of the body of the mandible is narrow and straight, with parallel edges. Posterior to the last tooth alveolus, the mandibular profile (best defined by the coronoid crest) curves slightly laterally from its longitudinal axis. The pan bone is inflated across the lower half of the mandibular body. In medial view (not figured), the mandibular fossa forms the posterior half of the preserved mandible (matrix and a layer of fiberglass cover the wall of the pan bone). The mandibular canal extends anteriorly from the mandibular fossa.

The mandibular condyle faces posterodorsally, with an articular face that is dorsoventrally elongate and spindle-shaped, narrowing dorsally. The ventral margin of the condyle is in line with the coronoid crest, directly posterior to the last dental alveolus.

Postcranial Material

The axis (C2) is more or less complete (Fig. 7A, Table 3); it is not clear if the dorsal part of the spinous process is missing or only poorly developed. The form of the axis is close to an equilateral triangle. In anterior view, the odontoid process is wide and relatively short anteroposteriorly. Each of the reniform anterior articular surfaces has a pitted texture, presumably for cartilage. The transverse process is relatively small, extending only a few millimeters lateral to the articular surface. The neural canal is roughly pentagonal and relatively open. The postzygapophyses are located near the dorsal end of the neural arch. In the posterior face, two well-developed cavities lateral to the vertebral body serve for the insertion of the spinalis muscle.

The third cervical vertebra (C3) (Fig. 7B, Table 3) is not fused with the axis. The vertebra is extremely compressed anteroposteriorly compared with the more posterior vertebrae associated with the specimen. In anterior view, the vertebral body is oval. The transverse process is oriented anteriorly and perforated by a transverse foramen. The transverse foramen is preserved complete only on the left; its shape is circular and it is positioned dorsally, near the neural arch. The right transverse foramen is an open notch, possibly because of damage during

← FIGURE 8. Strict consensus tree of the six shortest cladograms (1887 steps) showing the phylogenetic relationships of *Papahu taitapu* within Odontoceti. This tree was obtained by parsimony analysis of non-additive, equally weighted characters. Data matrix modified from Geisler et al. (2012).

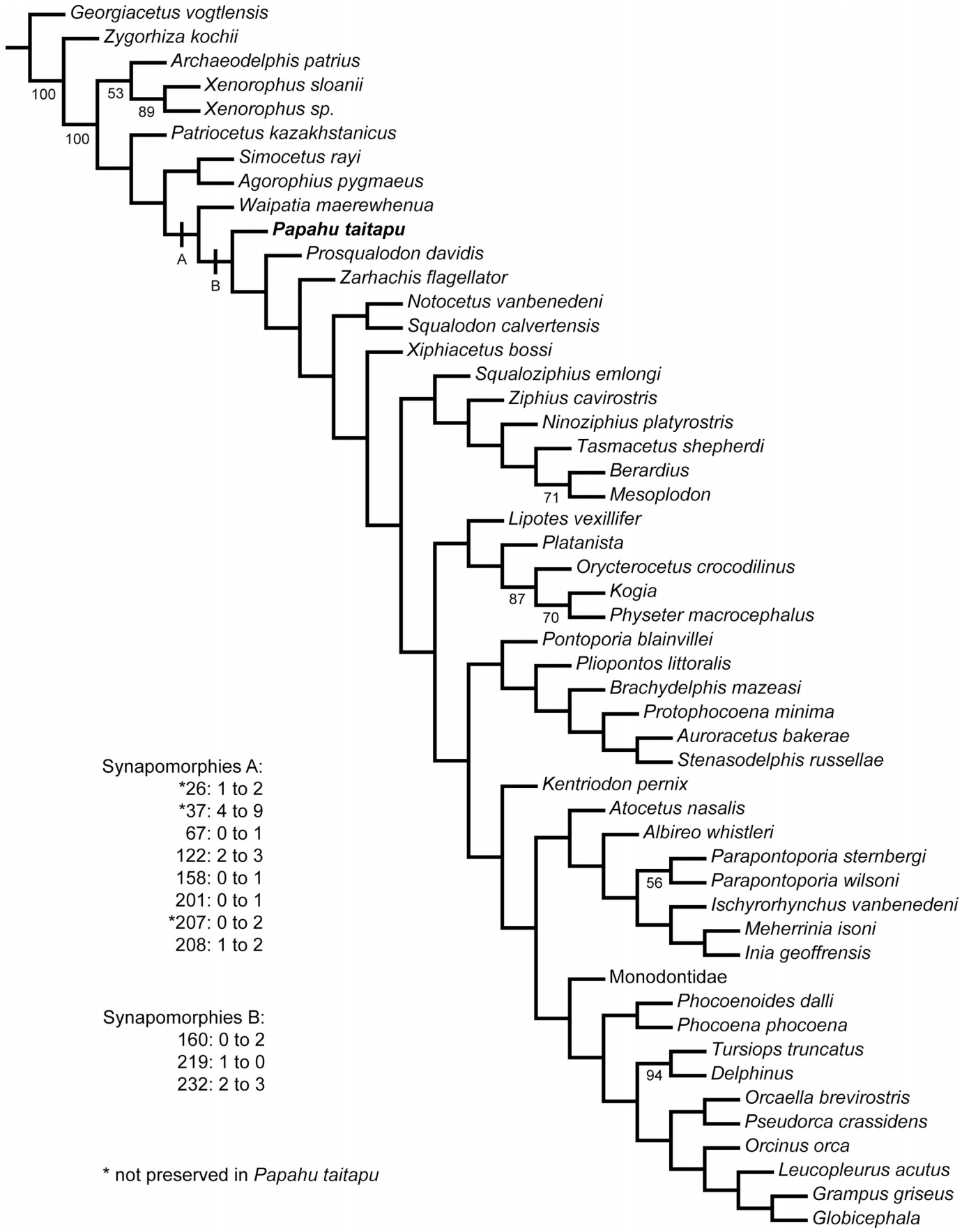
Georgiacetus vogtlensis
Zygorhiza kochii
Archaeodelphis patrius
Xenorophus sloanii
Xenorophus sp.
Patriocetus kazakhstanicus
Simocetus rayi
Agorophius pygmaeus
Waipatia maerewhenua
Papahu taitapu
Prosqualodon davidis
Zarhachis flagellator
Notocetus vanbenedeni
Squalodon calvertensis
Xiphiacetus bossi
Squaloziphius emlongi
Ziphius cavirostris
Ninoziphius platyrostris
Tasmacetus shepherdi
Berardius
Mesoplodon
Lipotes vexillifer
Platanista
Orycterocetus crocodilinus
Kogia
Physeter macrocephalus
Pontoporia blainvillei
Pliopontos littoralis
Brachydelphis mazeasi
Protophocoena minima
Auroracetus bakerae
Stenasodelphis russellae
Kentriodon pernix
Atocetus nasalis
Albireo whistleri
Parapontoporia sternbergi
Parapontoporia wilsoni
Ischyrorhynchus vanbenedeni
Meherrinia isoni
Inia geoffrensis
Monodontidae
Phocoenoides dalli
Phocoena phocoena
Tursiops truncatus
Delphinus
Orcaella brevirostris
Pseudorca crassidens
Orcinus orca
Leucopleurus acutus
Grampus griseus
Globicephala
100
53
89
100
A
B
71
87
70
56
94
Synapomorphies A:
*26: 1 to 2
*37: 4 to 9
67: 0 to 1
122: 2 to 3
158: 0 to 1
201: 0 to 1
*207: 0 to 2
208: 1 to 2
Synapomorphies B:
160: 0 to 2
219: 1 to 0
232: 2 to 3
* not preserved in Papahu taitapu

preparation. The neural canal is ovate and slightly smaller than the body. The prezygapophysis is well developed and faces ventrolaterally.

Other poorly preserved postcranial material includes a lumbar vertebra with low transverse processes and an almost complete spinous process (Fig. 7C, Table 3), two vertebrae with relatively long centra, and a slender thoracic rib with an anteroposteriorly compressed body and a reduced tuberculum and capitulum (greatest length of rib: 17 mm).

CLADISTIC ANALYSIS

Cladistic Results and Discussion

Non-additive, Equally Weighted Parsimony Analysis—The cladistic analysis using equal weights recovered six most parsimonious trees of 1887 steps each. In the consensus tree (Fig. 8), *Papahu taitapu* and other 'archaic' odontocetes (*Simocetus rayi*, *Prosqualodon davidis*, *Waipatia maerewhenua*, *Patriocetus kazakhstanicus*, and *Agorophius pygmaeus*) plot together in a polytomy of stem Odontoceti. Lack of resolution here, we suggest, reflects several issues, including (1) loss of type material and/or uncertainty about details of figured material (*P. davidis*, *A. pygmaeus*, *P. kazakhstanicus*); (2) limited or no access to details of character-rich tympanoperiotics and/or adjacent details of the basicranium (*P. davidis*, *A. pygmaeus*, *P. kazakhstanicus*, *S. emlongi*); and (3) limited taxonomic sampling of basal Odontoceti. All the taxa mentioned above (apart from *Papahu taitapu*) are so disparate that they have, in the past, been placed in separate families: Simocetidae, Prosqualodontidae, Waipatiidae, Patriocetidae, and Agorophiidae (see Fordyce and Muizon, 2001; Fordyce, 2002).

Parsimony Analysis under Implied Weighting—The analysis under implied weights (Fig. 9) recovered a single tree with a score of 147.43. The synapomorphies supporting the node that includes *Waipatia maerewhenua* and all other odontocetes crownwards (Fig. 9, node A) are the gap between the premaxillae anterior to the external bony nares is narrow (char. 67:1); the nasals are located in line with gap between postorbital process and the zygomatic process of squamosal or in line with the anterior tip of the latter (char. 122:3); the palatine is thick and forms part of the anterior wall of the choanae (char. 158:1); the anterior process of the periotic comes to a blunt apex (char. 201:1); and the shape of the cross-section of the anterior process of the periotic at midlength is roughly circular (char. 208:2).

The node that includes *Papahu taitapu* and all other odontocetes crownwards is supported by the following synapomorphies (Fig. 9, node B): the palatine is divided into medial and lateral lamina by a well-developed fossa (char. 160, scored as uncertain state 1 or 2); a rounded anteromedial corner of the pars cochlearis (char. 219:0); and the virtual absence of the dorsal edge of tegmen tympani (dorsal crest) (char. 232:3).

DISCUSSION

Ontogeny

The skeletal maturity of *Papahu taitapu* can be inferred using methods of developmental assessment for living delphinids, although some characters mentioned below (e.g., nuchal and temporal crests) may not be developed in adulthood in a particular species. We estimated skeletal maturity using the method proposed by Galatius (2010) of development of specific cranial sutures. All the selected sutures (squamosal-parietal, parietal-frontal, parietal-supraoccipital, parietal-exoccipital, and frontal-exoccipital) are partially or totally fused (score: 30–40). However, such high scores (>30) are attained and stabilized by the delphinid *Lagenorhynchus albirostris* relatively early (~7 years), whereas sexual maturity is reached in average at about 8.7 (females) to 11.6 (males) years (Kinze, 2008).

The application of another method of assessing skeletal maturity (Perrin, 1975) suggests that *Papahu taitapu* may be physically immature (classes IV–V of development of Perrin's (1975:42) scale), because of (1) the lack of prominent cranial crests (i.e., nuchal, temporal); (2) the smooth pitting (presumably for cartilage) of the articular process of the axis; (3) transverse processes of the axis are not completely fused ventromedially, exposing a small portion of the vertebral body in ventral view (not illustrated); (4) generally open and clear sutures on the skull; (5) the notochordal pit is evident in the cervical vertebrae; and (6) the vertebral epiphyses are not ankylosed to the extent that the suture is obliterated and the epiphyses are smaller than the respective vertebral centra.

Comparisons

The cladistic analysis provides a phylogenetic framework for the possible position of *Papahu taitapu* within Odontoceti. It is axiomatic that more could be done to resolve the relationships of fossil taxa, especially using new and better-preserved archaic cetaceans. For now, given the low branch support of many of the clades, we consider it premature to draw any conclusions on the overall phylogeny of odontocetes in general or, especially, to propose changes in taxonomy above the genus level. Other authors have discussed the relationships of some of these 'stem' or 'archaic' odontocetes, including the early work by Muizon (1984, 1987, 1988a, 1991, 1994) and other cladistic studies (e.g., Fordyce, 1994; Geisler and Sanders, 2003; Lambert, 2005; Barnes, 2006; Barnes et al., 2010; Geisler et al., 2011, 2012). A range of symplesiomorphies, and the real or preservational absence of evident synapomorphies that characterize other groups of odontocetes (involving, e.g., incomplete rostrum pterygoid fossae, and earbones), contribute to the position of *Papahu taitapu*. The absence of synapomorphies has affected the phylogenetic understanding of other groups, such as Dalpiazinidae (see Muizon, 1994; Barnes, 2006). The ranking of *Papahu taitapu* as incertae sedis signals the poor state of phylogenetic knowledge of stem Odontoceti, or 'archaic' odontocetes. The inclusion of more taxa into phylogenetic analyses, especially from poorly sampled time periods (such as the early Miocene), should improve the phylogenetic accuracy (May-Collado and Agnarsson, 2006; Agnarsson and May-Collado, 2008; Heath et al., 2008). Early Miocene odontocetes further deserve concerted field effort leading to new recoveries because of the global rarity of well-preserved and well-dated specimens in the range Aquitanian to middle Burdigalian, about 23–18 Ma.

In addition to the cladistic analysis (Figs. 7, 8), we performed a search of the literature looking for more fragmentary material named elsewhere that might be phenetically similar to, and possibly congeneric with, *Papahu taitapu*. Some comparisons are briefly stated in Diagnosis, and some below. Taxa reported for the early Miocene include the following families and key species (according to Fordyce and Muizon, 2001; Uhen, 2012): Allodelphinidae (*Allodelphis pratti* Wilson, 1935—see Barnes, 2006), Dalpiazinidae (*Dalpiazina ombonii* (Longhi, 1898)—see

← FIGURE 9. Single optimal tree (score = 147.43) showing the phylogenetic relationships of *Papahu taitapu* within Odontoceti. This cladogram was obtained by parsimony analysis of non-additive characters and implied weighting (k = 3) (Goloboff, 1993). Data matrix modified from Geisler et al. (2012).

Pilleri, 1985:pl. 49–52), Eoplatanistidae (*Eoplatanista italica* Dal Piaz, 1916b—see Pilleri, 1985:pl. 68–69, and Muizon, 1988b), Eurhinodelphinidae (*Ziphiodelphis abeli* Dal Piaz, 1908—see Lambert, 2005), Kentriodontidae (*Kentriodon pernix* Kellogg, 1927), stem Physeteroidea sensu Lambert, 2008 (*Eudelphis mortezelensis* du Bus, 1872), Squalodelphinidae (*Squalodelphis fabianii* Dal Piaz, 1916a—see Pilleri, 1985:pl. 25–26; *Notocetus vanbenedeni* Moreno, 1892), Prosqualodontidae (*Prosqualodon davidis* Flynn, 1923—see Cozzuol, 1996), and Squalodontidae (*Squalodon bariensis* (Jourdan, 1861)—see Pilleri, 1985:pl. 1–5, and Muizon, 1991).

Comparisons with Allodelphinidae—Wilson (1935) included *Allodelphis* in Delphinidae, but Fordyce and Muizon considered it Platanistoidea incertae sedis. Barnes (2006) created the monotypic family Allodelphinidae, and Barnes and Reynolds (2009) established the genus *Zarhinocetus*. Comparisons with Allodelphinidae are difficult because this family is mainly diagnosed based on aspects of the rostrum that are not preserved in *Papahu taitapu*; some other characters, such as the elevated nuchal crest and fusion of premaxilla and maxilla, may have some ontogenetic influence. *Papahu taitapu* resembles the known genera of Allodelphinidae in superficial features, such as the relative size of the skull and homodonty, but differs from Allodelphinidae in the following: the nasals are not elongate and narrow; the facial region near the vertex of the skull is not elevated in sagittal plane; the posterolateral sulcus is prominent; the proximal end of each premaxilla is divided into a splint and plate, and is not thin, narrow, and feathered; and the nuchal crest is not anteroposteriorly thick and elevated.

Comparisons with Prosqualodontidae, Squalodontidae, and Dalpiazinidae—The relationships of Squalodontidae and other Platanistoidea have been discussed elsewhere (of note, Muizon, 1991). Dalpiazinidae, a monogeneric family typified by *Dalpiazina* Muizon, 1988b, is tentatively considered a sister group to Squalodontidae (Muizon, 1991), and needs review using computer-assisted cladistics. Prosqualodontidae Cozzuol, 1996, is a monogeneric family for *Prosqualodon* only. Alternatively, the genus *Prosqualodon* may belong to Squalodontidae (Fordyce and Muizon, 2001). Diagnostic characters for Prosqualodontidae, Squalodontidae, and Dalpiazinidae that are not preserved in *Papahu taitapu* include apex of rostrum formed by premaxilla and lengthening of rostrum and widening of its apex. *Papahu taitapu* shares with Dalpiazinidae, Squalodontidae, and Prosqualodontidae the presence of a 'vomerian window' (ventral exposure of the vomer on the rostrum, also present in Waipatiidae and stem Physeteroidea), but the degree of exposure in *Papahu taitapu* is unknown because the rostrum is ventrally eroded. *Papahu* resembles *Dalpiazina,* but differs from Prosqualodontidae and Squalodontidae in features including inferred homodonty and plate-like nasals overhanging the nares.

Comparisons with Squalodelphinidae—*Papahu taitapu* differs from the members of the family Squalodelphinidae in the absence of a square-shaped pars cochlearis, but resembles Squalodelphinidae in the presence of a large and thin-edged dorsal opening of the cochlear aqueduct. The family Squalodelphinidae is diagnosed by the following characters not preserved in *Papahu taitapu*: ventral groove along the whole length of the tympanic bulla; apical extension of the manubrium of the malleus; and strong development of the dorsal transverse process and reduction of the ventral transverse process of the atlas. The absence of the coracoid process in the scapulae of Platanistidae and Squalodelphinidae cannot be compared in *Papahu taitapu*. The probably diagnostic 'subcircular fossa' (sensu Muizon, 1987) of Platanistidae, Squalodelphinidae, and Waipatiidae (see Fordyce, 1994) is not present in *Papahu taitapu*.

Comparisons with Eurhinodelphinidae and Eoplatanistidae—Eurhinodelphinidae and the monogeneric family Eoplatanistidae were interpreted as Superfamily Eurhinodelphinoidea, a sister taxon of Delphinida, according to Muizon (1991). A more recent cladistic analysis suggests that eurhinodelphinids are more closely related to ziphiids than to delphinidans (Lambert, 2005). *Eoplatanista* was not included in the latter analysis, however, and more research is needed to clarify relationships of Eurhinodelphinidae and Eoplatanistidae. *Papahu taitapu* shares with Eurhinodelphinoidea the presence of homodonty, but differs from Eurhinodelphinidae in the absence of orbital and temporal extensions of the pterygoid sinus complex; the presence of a mesorostral groove that is not roofed by the premaxillae; the lack of a strong inflexion of the premaxillae to the vertex; and the lack of an anteroposteriorly thickened postglenoid process. *Papahu taitapu* resembles Eurhinodelphinidae in the presence of a prominent fissure in the premaxillary-maxillary suture (also present in Allodelphinidae) and a relatively robust zygomatic process of the squamosal. The rostrum of *Papahu taitapu* is lost, making impossible to compare some of the most frequently cited diagnostic characters of Eurhinodelphinidae, such as the very long rostrum that extends anterior to the apex of the mandible, and the sharp ventral keel at the level of the hamular process.

Comparisons with Stem Physeteroidea—*Papahu taitapu* differs from *Eudelphis* and other physeteroids in the absence of a supracranial basin; asymmetric bony nares; and asymmetric premaxillae.

Comparisons with Kentriodontidae—*Papahu taitapu* shares a key character that Muizon (1988a) regarded as only present in Delphinida: the duplication of the palatine into medial and lateral laminae. However, the presence of a lateral lamina of the palatine was also indicated for the following non-delphinidans by Geisler et al. (2012): *Prosqualodon davidis*, *Squaloziphius emlongi* (contra Muizon, 1991), and *Zarhachis flagellator*. The following diagnostic characters of Delphinida are not preserved in *Papahu taitapu*: loss of lateral lamina of the pterygoid, excavation of posterodorsal region of involucrum of tympanic bulla to form a saddle-shaped profile; development of processus muscularis of malleus; and the enlarged transverse apophysis on lumbar vertebrae.

Functional Anatomy

Papahu taitapu is unexceptional within the Odontoceti in terms of inferred functional morphology. The body size of *Papahu taitapu* can be inferred using Pyenson and Sponberg's (2011) formula for stem Platanistoidea: $\log(L) = 0.92 \times (\log(BIZYG) - 1.51) + 2.49$, where byzygomatic width (BIZYG) is 18.2 cm. The resulting approximate total length of *Papahu taitapu* is 1.8 m, comparable to small living delphinids of the genera *Sotalia*, *Delphinus*, and *Stenella*. The species currently plots as a stem odontocete, which limits functional inference based on phylogenetic position, but osteological correlates of soft tissues in extant odontocetes help to assess functional complexes.

In the respiratory system, *Papahu taitapu* is intermediate between cetaceans with elongated nasals and forward-placed blowhole(s) (e.g., archaeocetes, some 'archaic' odontocetes) and odontocetes with nodular, anteroposteriorly compressed nasals and posteriorly placed vertical narial passages (e.g., Delphinidae). In terms of respiratory structures implicated in echolocation, there is no direct evidence for nasal diverticula (epicranial sinuses) other than the premaxillary sac, which has a distinct fossa and associated premaxillary foramen (one foramen normally in crown odontocetes, two in *Papahu taitapu*). The multiple dorsal infraorbital foramina at the premaxillary-maxillary suture and in the maxilla on the base of the rostrum (forward of the antorbital notches) suggest heavily vascularized and innervated facial soft tissues, with a significant origin for the rostral part of the nasofacial muscles, such as the rostral and nasal plug muscles (Mead, 1975). The facial fossa behind the antorbital notches formed an

origin for the nasofacial muscles, but size and shape of soft tissues is uncertain. The antorbital notches show slight but clear directional asymmetry, with the left antorbital notch more open than the right. Such asymmetry at the notches is evident in many living odontocetes and in fossils (e.g., *Waipatia maerewhenua*), and is consistent with the presence of asymmetrical nasofacial tissues (Mead, 1975; Heyning, 1989). The rostrum is too incomplete to make useful inference on feeding habits. Likewise, although the orbit is well preserved, orbital patterns of soft tissues-to-bone are too poorly known in modern odontocetes to interpret structures in *Papahu taitapu*.

Pterygoid sinuses occur in living odontocetes and mysticetes, partly or wholly developed in bony sinus fossae on the basicranium. The exact function of the sinuses is uncertain but, in extant odontocetes, the sinuses are generally implicated in acoustic isolation for echolocation (Fraser and Purves, 1960; Norris, 1968). *Papahu taitapu* shows a relatively basic stage in the development of the pterygoid sac system, with evidence of a main fossa preserved on the alisphenoid, an anterior extension into the pterygoid hamulus, and no evidence of invasion of the orbits. The same grade of development is shared with *Waipatia maerewhenua*, differing from Squalodelphinidae and Platanistidae in the lack of orbital extensions of the pterygoid sinus (Fordyce, 1994).

ACKNOWLEDGMENTS

We thank all those who helped in many ways: O. Lambert and C. Gutstein reviewed this manuscript and provided useful comments; S. White for advice on Māori language and its application to the fossil; F. G. Marx for help using TNT and comments on an earlier version of the manuscript; A. Grebneff for field work and skilful preparation; J. Geisler and collaborators for making available the data matrix used here, and J. Geisler for discussions on character descriptions and scorings. This article forms part of G. Aguirre's Ph.D. dissertation, supported by a Doctoral Scholarship from the University of Otago. Field work was supported by research funds from the Department of Geology, University of Otago.

LITERATURE CITED

Agnarsson, I., and L. J. May-Collado. 2008. The phylogeny of Cetartiodactyla: the importance of dense taxon sampling, missing data, and the remarkable promise of cytochrome *b* to provide reliable species-level phylogenies. Molecular Phylogenetics and Evolution 48:964–985.

Barnes, L. G. 1985. The late Miocene dolphin *Pithanodelphis* Abel, 1905 (Cetacea: Kentriodontidae) from California. Contributions in Science, Natural History Museum of Los Angeles County 367: 1–27.

Barnes, L. G. 2006. A phylogenetic analysis of the superfamily Platanistoidea (Mammalia, Cetacea, Odontoceti). Beiträge zur Paläontologie 30:25–42.

Barnes, L. G., T. Kimura, and S. J. Godfrey. 2010. The evolutionary history and phylogenetic relationships of the Superfamily Platanistoidea; pp. 445–488 in M. Ruiz-García and J. M. Shostell (eds.), Biology, Evolution and Conservation of River Dolphins within South America and Asia. Nova Science Publishers, New York.

Bianucci, G., and W. Landini. 2002. Change in diversity, ecological significance and biogeographical relationships of the Mediterranean Miocene toothed whale fauna. Geobios 24:19–28.

Bishop, D. G. 1968. Geologic map of Kahurangi, New Zealand. 1:63360. New Zealand Geological Survey Sheet S2.

Bremer, K. 1994. Branch support and tree stability. Cladistics 10:295–304.

Brisson, M. J. 1762. Regnum animale in classes IX. distributum, sive synopsis methodica sistens generalem animalium distributionem in classes IX, & duarum primarum classium, quadrupedum scilicet & cetaceorum, particularem divisionem in ordines, sectiones, genera & species. Cum brevi cujusque speciei descriptione, citationibus auctorum de iis tractantium, nominibus eis ab ipsis & nationibus impositis, nominibusque vulgaribus. Theodorum Haak, Lugduni Batavorum [Leiden], 296 pp.

Cione, A. L., M. A. Cozzuol, M. T. Dozo, and C. Acosta Hospitaleche. 2011. Marine vertebrate assemblages in the southwest Atlantic during the Miocene. Biological Journal of the Linnean Society 103:423–440.

Cooper, R. A. (ed.). 2004. New Zealand Geological Timescale, Volume 22. Institute of Geological and Nuclear Sciences, Lower Hutt, 284 pp.

Cozzuol, M. A. 1996. The record of the aquatic mammals in southern South America. Münchner Geowissenschaftliche Abhandlungen 30:321–342.

Dal Piaz, G. 1908. Sui vertebratei delle arenarie mioceniche di Belluno. Atti Della Accademia Scientifica Vento-Trentino-istriana 5:106–120.

Dal Piaz, G. 1916a. Gli Odontoceti del Miocene Bellunese. Parte Terza, *Squalodelphis fabianii*. Memorie dell'Istituto Geologico della R. Universitá di Padova 5:1–28.

Dal Piaz, G. 1916b. Gli Odontoceti del Miocene Bellunense. Parte Quarta, *Eoplatanista italica*. Memorie dell'Istituto Geologico della Universitá di Padova 5:1–23.

du Bus, B. A. L. 1872. Mammifères noveaux du crag d'Anvers. Bulletin de l'Académie des Sciences de Belgique 34:491–509.

Flower, W. H. 1867. IV. Description of the skeleton of *Inia geoffrensis* and of the skull of *Pontoporia blainvillii*, with remarks on the systematic position of these animals in the Order Cetacea. Transactions of the Zoological Society of London 6:87–116.

Fordyce, R. E. 1991. A new look at the fossil vertebrate record of New Zealand; pp. 1191–1316 in P. V. Rich, J. M. Monaghan, R. F. Baird, and T. H. Rich (eds.), Vertebrate Palaeontology of Australasia. Pioneer Design Studio and Monash University, Melbourne.

Fordyce, R. E. 1994. *Waipatia maerewhenua*, new genus and new species (Waipatiidae, new family), an archaic late Oligocene dolphin (Cetacea: Odontoceti: Platanistoidea) from New Zealand; pp. 147–176 in A. Berta and T. Deméré (eds.), Contributions in Marine Mammal Paleontology Honoring Frank C. Whitmore, Jr. Proceedings of the San Diego Society of Natural History 29.

Fordyce, R. E. 2002. *Simocetus rayi* (Odontoceti: Simocetidae, new family): a bizarre new archaic Oligocene dolphin from the Eastern North Pacific; pp. 185–222 in R. J. Emry (ed.), Cenozoic Mammals of Land and Sea: Tributes to the Career of Clayton E. Ray. Smithsonian Institution Press, Washington, D.C.

Fordyce, R. E., and C. de Muizon. 2001. Evolutionary history of whales: a review; pp. 169–234 in J.-M. Mazin and V. de Buffrenil (eds.), Secondary Adaptation of Tetrapods to Life in Water. Proceedings of the International Meeting, Poitiers, 1996. Verlag Dr Friedriech Pfeil, Munich.

Fraser, F. C., and P. E. Purves. 1960. Hearing in cetaceans: evolution of the accessory air sacs and structure of the outer and middle ear in recent cetaceans. Bulletin of the British Museum (Natural History), Zoology 7:1–140.

Galatius, A. 2010. Paedomorphosis in two small species of toothed whales (Odontoceti): how and why? Biological Journal of the Linnean Society 99:278–295.

Geisler, J. H., and A. E. Sanders. 2003. Morphological evidence for the phylogeny of Cetacea. Journal of Mammalian Evolution 10: 23–129.

Geisler, J. H., S. J. Godfrey, and O. Lambert. 2012. A new genus and species of late Miocene inioid (Cetacea, Odontoceti) from the Meherrin River, North Carolina, U.S.A. Journal of Vertebrate Paleontology 32:198–211.

Geisler, J. H., M. R. McGowen, G. Yang, and J. Gatesy. 2011. A supermatrix analysis of genomic, morphological, and paleontological data from crown Cetacea. BMC Evolutionary Biology 11:112.

Goloboff, P. A. 1993. Estimating character weights during tree search. Cladistics 9:83–91.

Goloboff, P. A., J. S. Farris, and K. C. Nixon. 2008. TNT, a free program for phylogenetic analysis. Cladistics 24:774–786.

Goloboff, P. A., J. S. Farris, M. Källersjö, B. Oxelman, M. J. Ramírez, and C. A. Szumik. 2003. Improvements to resampling measures of group support. Cladistics 19:324–332.

Gordon, D. P., I. G. Stuart, and J. D. Collen. 1994. Bryozoan fauna of the Kaipuke Siltstone, Northwest Nelson: a Miocene homologue of the modern Tasman Bay coralline bryozoan grounds. New Zealand Journal of Geology and Geophysics 37:239–247.

Heath, T. A., S. M. Hedtke, and D. M. Hillis. 2008. Taxon sampling and the accuracy of phylogenetic analyses. Journal of Systematics and Evolution 46:239–257.

Heyning, J. E. 1989. Comparative facial anatomy of beaked whales (Ziphiidae) and systematic revision among the families of extant Odontoceti. Contributions in Science, Natural History Museum of Los Angeles County 405:1–64.

Hollis, C. J., A. G. Beu, J. S. Crampton, M. P. Crundwell, H. E. G. Morgans, J. I. Raine, C. M. Jones, and A. F. Boyes. 2010. Calibration of the New Zealand Cretaceous-Cenozoic Timescale to GTS2004. GNS Science Report 43:1–20.

Jourdan, C. 1861. Description de restes fossiles de deux grands mammifères constituant deux genres, l'un le genre *Rhizoprion* de l'ordre des cétacés et du groupe des delphinoides; l'autre le genre *Dynocyon* de l'ordre des carnassiers et de la famille canidés. Annales de Science Naturelles, Zoologie 4:369–374.

Kellogg, A. R. 1927. *Kentriodon pernix*, a Miocene porpoise from Maryland. Proceedings of the United States National Museum 69(19):1–55.

Kellogg, A. R. 1928. The history of whales, their adaptation to life in the water (concluded). Quarterly Review of Biology 3:174–208.

Kellogg, A. R. 1932. A Miocene long-beaked porpoise from California. Smithsonian Miscellaneous Collections 87(2):1–11.

Kinze, C. C. 2008. White-Beaked Dolphin *Lagenorhynchus albirostris*; pp. 1255–1258 in W. F. Perrin, B. Würsig, and J. G. M. Thewissen (eds.), Encyclopedia of Marine Mammals. Academic Press, San Diego.

Lambert, O. 2005. Phylogenetic affinities of the long-snouted dolphin *Eurhinodelphis* (Cetacea, Odontoceti) from the Miocene of Antwerp, Belgium. Palaeontology 48:653–679.

Lambert, O. 2008. Sperm whales from the Miocene of the North Sea: a re-appraisal. Bulletin de l'Institut Royal des Sciences Naturelles de Belgique, Sciences de la Terre 78:277–316.

Lee, Y.-N., H. Ichishima, and D. K. Choi. 2012. First record of a platanistoid cetacean from the middle Miocene of South Korea. Journal of Vertebrate Paleontology 32:231–234.

Longhi, P. 1898. Sopra i resti di un cranio di *Champsodelphis* fossile scoperto nella molassa miocenica del Bellunese: Memoria. Atti della Societa Veneto-Trentina di Scienze Naturali Residente in Padova 3:1–59.

Marx, F. G., and M. D. Uhen. 2010. Climate, critters, and cetaceans: Cenozoic drivers of the evolution of modern whales. Science 327:993–996.

May-Collado, L., and I. Agnarsson. 2006. Cytochrome b and Bayesian inference of whale phylogeny. Molecular Phylogenetics and Evolution 38:344–354.

Mead, J. G. 1975. Anatomy of the external nasal passages and facial complex in the Delphinidae (Mammalia: Cetacea). Smithsonian Contributions to Zoology 207:1–72.

Mead, J. G., and R. E. Fordyce. 2009. The therian skull: a lexicon with emphasis on the odontocetes. Smithsonian Contributions to Zoology 627:1–248.

Moreno, F. P. 1892. Noticias sobre algunos cetáceos fósiles y actuales de la República Argentina. Revista del Museo de La Plata 3:381–400.

Muizon, C. de. 1984. Les vertébrés fossiles de la Formation Pisco (Pérou). Deuxième partie: les odontocètes (Cetacea, Mammalia) du Pliocène inférieur de Sud-Sacaco. Travaux de l'Institut Français d'Etudes Andines 50:1–188.

Muizon, C. de. 1987. The affinities of *Notocetus vanbenedeni*, an early Miocene platanistoid (Cetacea, Mammalia) from Patagonia, Southern Argentina. American Museum Novitates 2904:1–27.

Muizon, C. de. 1988a. Les relations phylogénétiques des Delphinida (Cetacea, Mammalia). Annales de Paléontologie 74:159–227.

Muizon, C. de. 1988b. Le polyphylétisme des Acrodelphidae, odontocètes longisrostres du Miocène européen. Bulletin du Muséum National d'Histoire Naturelle, Paris, section C, série 4 10:31–88.

Muizon, C. de. 1991. A new Ziphiidae (Cetacea) from the early Miocene of Washington State (USA) and phylogenetic analysis of the major groups of odontocetes. Bulletin du Muséum National d'Histoire Naturelle, Paris, section C, série 4 12:279–326.

Muizon, C. de. 1994. Are squalodonts related to the platanistoids?; pp. 135–146 in A. Berta and T. A. Deméré (eds.), Contributions in Marine Mammal Paleontology Honoring Frank Whitmore, Jr. Proceedings of the San Diego Society of Natural History 29.

Murakami, M., C. Shimada, Y. Hikida, and H. Hirano. 2012. A new basal porpoise, *Pterophocaena nishinoi* (Cetacea, Odontoceti, Delphinoidea), from the upper Miocene of Japan and its phylogenetic relationships. Journal of Vertebrate Paleontology 32:1157–1171.

Nathan, S., H. J. Anderson, R. A. Cook, R. H. Herzer, R. H. Hoskins, J. I. Raine, and D. Smale. 1986. Cretaceous and Cenozoic Sedimentary Basins of the West Coast Region, South Island, New Zealand. New Zealand Geological Survey Basin Studies 1:1–90.

Norris, K. S. 1968. The evolution of acoustic mechanisms in odontocete cetaceans; pp. 297–324 in E. T. Drake (ed.), Evolution and Environment, A Symposium Presented on the Occasion of the One Hundredth Anniversary of the Foundation of Peabody Museum of Natural History at Yale University. Yale University Press, New Haven.

Pilleri, G. 1985. The Miocene Cetacea of the Belluno Sandstones (Eastern Southern Alps). Memorie di Scienze Geologische già Memorie degli Istituti di Geologia e Mineralogia dell'Università di Padova 36:1–250.

Perrin, W. F. 1975. Variation of spotted and spinner porpoise (genus *Stenella*) in the eastern Pacific and Hawaii. Bulletin of the Scripps Institution of Oceanography 21:1–206.

Pyenson, N., and S. Sponberg. 2011. Reconstructing body size in extinct crown Cetacea (Neoceti) using allometry, phylogenetic methods and tests from the fossil record. Journal of Mammalian Evolution 18:269–288.

Rattenbury, M. S., R. A. Cooper, and M. R. Johnston. 1998. Geology of the Nelson area. Institute of Geological and Nuclear Sciences 1:250,000 Geological Map 9:1–67, map.

Uhen, M. D. 2012. Online systematics archive 9, Cetacea [parameters: early Miocene, Odontoceti]. Available at www.pbdb.org. Accessed August 22, 2012.

Uhen, M. D., and N. D. Pyenson. 2007. Diversity estimates, biases, and historiographic effects: resolving the cetacean diversity in the Tertiary. Palaeontologia Electronica 10:1–22.

Uhen, M. D., R. E. Fordyce, and L. G. Barnes. 2008. Odontoceti; pp. 566–606 in C. M. Janis, G. F. Gunnell, and M. D. Uhen (eds.), Evolution of Tertiary Mammals of North America, Volume 2, Small Mammals, Xenarthrans, and Marine Mammals. Cambridge University Press, New York.

Wilson, L. E. 1935. Miocene marine mammals from the Bakersfield region, California. Bulletin of the Peabody Museum of Natural History, Yale University 4:1–14.

Wellman, H. W., A. C. Beck, D. Kear, R. P. Suggate, and G. W. Grindley. 1981. Stratigraphic columns for the Cretaceous-lower Quaternary sediments of North-West Nelson and the West Coast, South Island. New Zealand Geological Survey Report 63:1–102.

Submitted October 12, 2012; revisions received March 10, 2013; accepted April 10, 2013.

Handling editor: Erich Fitzgerald.